Modélisation par champ de phase des évolutions microstructurales dans les matériaux

Phase Field Model for Microstructure Evolution

L. THUINET
UMET, Université de Lille, CNRS, INRA, ENSCL
59655 Villeneuve d' Ascq

Ecole ModMat, 21 juillet 2015

Université de Lille

cnrs dépasser les frontières

UMET
Unité Matériaux Et Transformations

From one example …

Simulation of the precipitation of γ' precipitates inside Ni-based superalloys by phase field modeling

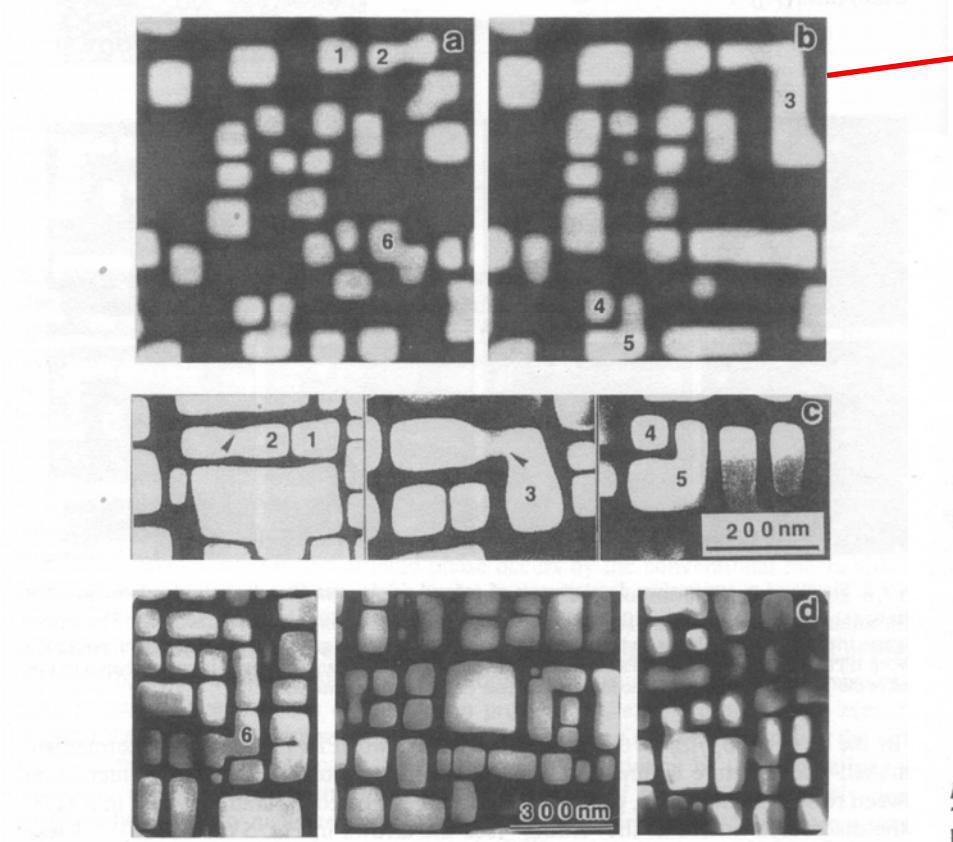

Figure 7. Comparison between the simulation predictions and experimental observations. (a)-(b) Repeats Fig. 6 (c) and (d). (c)-(d) Dark field TEM images showing the aligned precipitates with "odd" shapes in Ni-9.5Al-5.4Mo (Courtesy of G. Kostorz [80]).

Simulated results

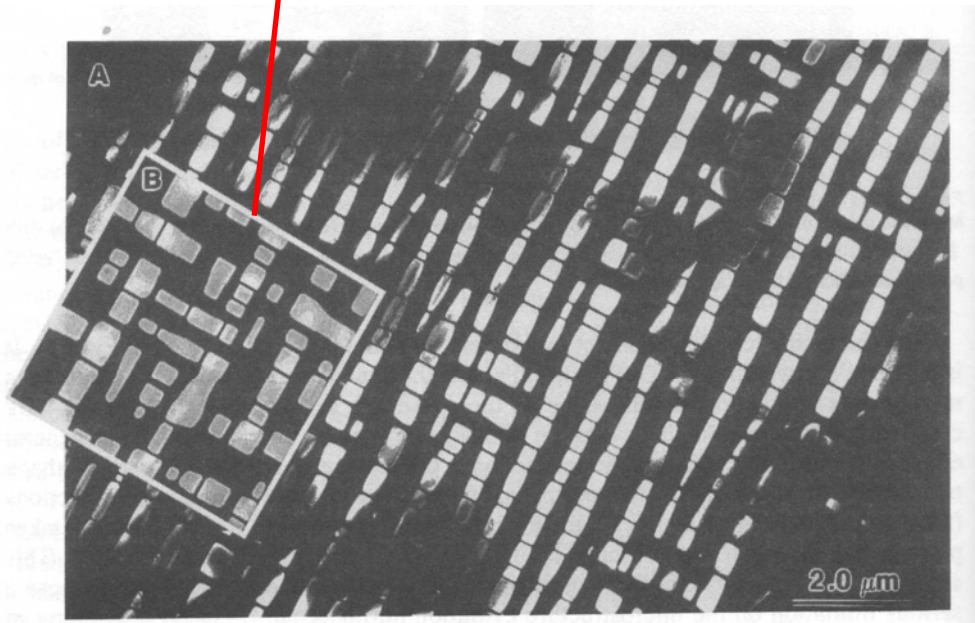

Figure 12. Comparison between experimental observation (a) (TEM micrograph of Ni-Al-Mo aged 2330 h at 775 °C (courtesy of M. Fährmann [86])) and simulation prediction (b) of discontinuous rafting structure in Ni-based superalloys. The edge length of the simulated micrograph is about 1.6 μm.

From Y. Wang, L. Q. Chen and A.G. Khachaturyan, Comp Sim in Mat Science, Kichner et al Ed. Nato Series 1996

… to general considerations

✓Phase field (PF) model is a powerful tool to simulate at the mesoscale (from nm to micron) the microstructure formation and evolution, in terms of :

- The size of the precipitates
- The shape of the precipitates
- The spatial distribution of the precipitates (alignment along specific crystallographic directions, …)

✓More generally, phase field model is applied to treat any compositional or structural inhomogeneities that arise during processing of materials: precipitates, dislocation loops, grain boundaries, cavities, bubbles, …

✓Important to understand the mechanisms lying behind these microstructural features, since they may have a detrimental impact on the mechanical properties of the materials

✓Due to its mesoscopic nature, phase field models are at:

•The mesoscopic/microscopic interface:

Phase field models require input data from atomistic simulations such as elastic constants, interfacial free energies, diffusion coefficients, chemical free energies, elastic misfits…

•The mesoscopic/macroscopic interface:

Knowledge of the microstructure to calculate macroscopic quantities (porosity, thermal conductivities, …)

Plan

✓Phase field formalism

•Description of the microstructure

•Thermodynamics

•Kinetics

•Advantages and limitations

✓Applications

Phase Field Formalism

Description of the microstructure

✓ What is it?

The ensemble of defects that are in thermodynamic equilibrium or not. Their number and topology evolve with time in order to reach the minimum of the thermodynamic potential adopted. Both the compositional /structural domains and also interfaces has to be correctly described as a whole by using a set of field variables.

✓How can it be described ?

There are two kinds of field variables - or order parameters -, conserved and not conserved.

•Conserved parameters (obeys to a conservation law, like diffusion equation):
Most of the time, composition of the different diffusing species

•Non conserved parameters:
LRO parameters which charaterize the cristallinity of the different phases

Given the values of the order parameters at each place and time, the microstructure is totally described.

Description of interfaces

✓The order parameters are continuous across the interfacial regions, and hence the interfaces are diffuse.

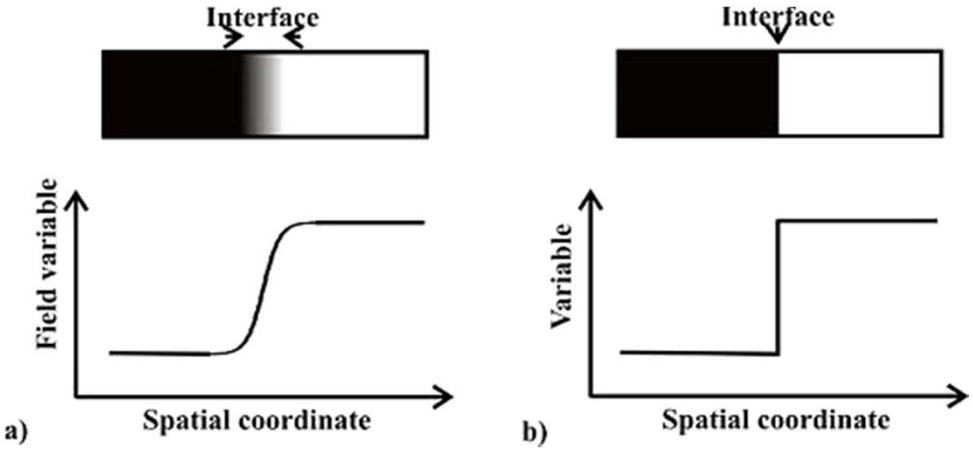

a) Diffuse interface (PF), b) sharp interface

✓In conventional approaches, regions separating compositional or structural domains are treated as mathematically sharp interfaces. This involves the explicit tracking of the interface positions, which is impractical for complicated 3D microstructures

✓The tracking of the interfaces in phase field models is automatically incorporated in the evolution equations thanks to the diffuse nature of the interfaces, which allows the treatment of any microstructures

✓ Example 1: many-variant solid phase transformation

In the case of γ hydride precipitation, three structural order parameters may be associated to the three equivalent orientations of the precipitates with respect to the matrix. Non conserved order parameters are therefore introduced: $\eta_1(\mathbf{r},t)$, $\eta_2(\mathbf{r},t)$, $\eta_3(\mathbf{r},t)$

$\eta_i(\mathbf{r},t) = 0$ if there is matrix in $(\mathbf{r},t)$

$\eta_i(\mathbf{r},t) = \pm 1$ if there is hydride variant i in $(\mathbf{r},t)$

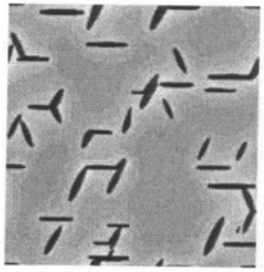

(From Ma et al, JNM, 2002)

c(**r**,t), the H concentration field, is a conserved order parameter (directly related to the H mass) that may describe non homogeneous situations.

✓ Example 2: gas bubble kinetics under irradiation

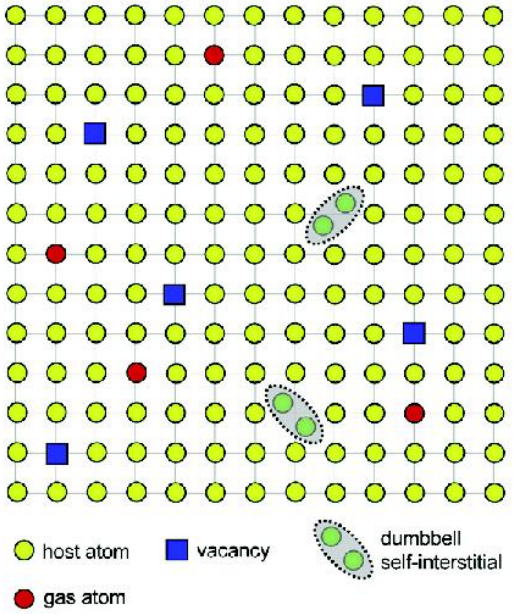

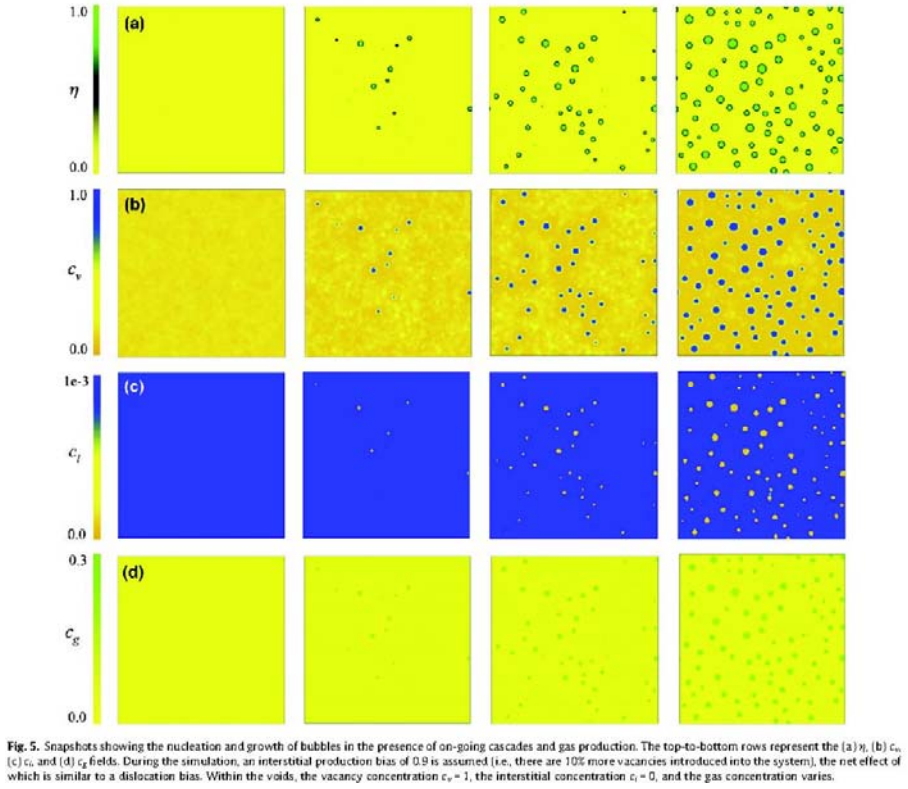

Fig. 5. Snapshots showing the nucleation and growth of bubbles in the presence of on-going cascades and gas production. The top-to-bottom rows represent the (a) η, (b) c_v, (c) c_i, and (d) c_g fields. During the simulation, an interstitial production bias of 0.9 is assumed (i.e., there are 10% more vacancies introduced into the system), the net effect of which is similar to a dislocation bias. Within the voids, the vacancy concentration $c_v = 1$, the interstitial concentration $c_i = 0$, and the gas concentration varies.

(From Millet et al, Comp. Mat. Science, 2011)

Order parameters required: local composition of vacancies $c_v(\mathbf{r},t)$, self-interstitials $c_i(\mathbf{r},t)$, gas $c_g(\mathbf{r},t)$ (conserved) + $\eta(\mathbf{r},t)$ which distinguishes solid and voids (non conserved)

+ set of order parameters $\phi_{1\rightarrow p}$ to represent crystallographic grain orientations for polycristalline simulations

+ …

The importance of thermodynamics

✓ Shows the way

The equilibrium final state of the system corresponds to the minimum of the thermodynamic potential with respect to the extensive internal variables. In condensed matter it is usual to work at constant volume and temperature and therefore the free energy F is the thermodynamic potential. Taking into account the spatial range of the interactions (SR = Short Range, LR = Long Range), two different kinds of contributions can be considered

$$F = F_{SR} + F_{LR}$$

The main differences among phase field models lie in the treatment of various contributions to the total free energy (elastic energy, electrostatic energy, magnetic energy,...)

✓All the different contributions must be expressed as function of the set of order parameters used to describe the microstructure

✓Short range chemical and structural contribution F_{SR}:

$c_1, \ldots, c_n$: conserved order parameters

$\eta_1, \ldots, \eta_n$: non conserved order parameters

$$F_{SR} = \int_{V_m} \left[f_{hom}(c_1, c_2, \ldots, c_n, \eta_1, \eta_2, \ldots, \eta_p) + \sum_{i=1}^{n} \frac{\alpha_i}{2}(\nabla c_i)^2 + \sum_{j=1}^{p} \frac{\beta_j}{2}(\nabla \eta_j)^2 \right] dV$$

f_{hom}: local free-energy density which incorporates local contribution from short-range chemical interactions

Gradient energy terms which are nonzero only at and around interfaces, related to the interfacial energy

α_i, β_j: stiffness coefficients

Local free energy density function f_{hom}

✓Example 1: double-well polynomial

Used to treat the simple mixture of two phases in equilibrium :

$$f_{\text{hom}}(c) = A\left[-\tfrac{1}{2}(c(\vec{r},t)-\bar{c})^2 + \tfrac{1}{\Delta c^2}(c(\vec{r},t)-\bar{c})^4\right] = A\tilde{f}_{\text{hom}}(c)$$

$\Delta c = c_2 - c_1 \quad \bar{c} = (c_1 + c_2)/2$

The two minima of the function are c_1 and c_2 and correspond to the equilibrium compositions of the phases

A is the energy scale and can be calibrated on the nucleation driving force of the system

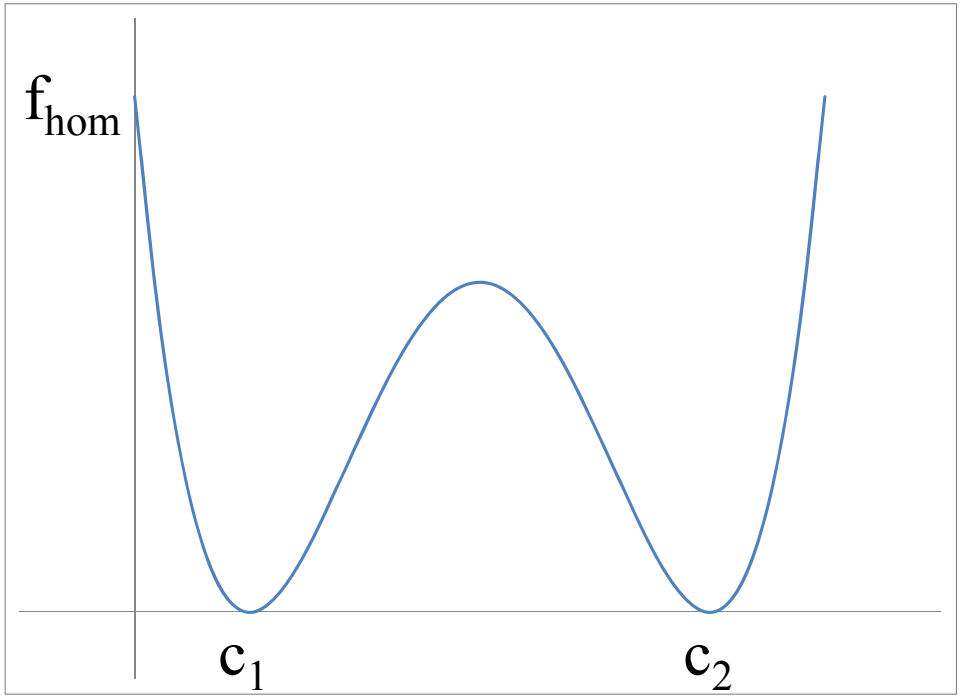

✓Example 2: Ginzburg-Landau expression

For many-solid phase transformations, the free energy volume density $f(c,\eta_i)$ has to satisfy a given number of symmetry conditions. In the case of hydrides precipitation in a Zr matrix Ma *et al.* (Script. Met. 2002) devised a Ginzburg-Landau like expression:

$$f(c,\eta_1,\eta_2,\eta_3)=\frac{A_1}{2}(c-c_1)^2+\frac{A_2}{2}(c-c_2)\sum_{i=1}^{3}\eta_i^2-\frac{A_3}{4}\sum_{i=1}^{3}\eta_i^4+\frac{A_4}{6}\sum_{i=1}^{3}\eta_i^6+$$

$$A_5\sum_{i\neq j}\eta_i^2\eta_j^2+A_6\sum_{i\neq j\neq k}\eta_i^4\left(\eta_j^2+\eta_k^2\right)+A_7\sum_{i\neq j\neq k}\eta_i^2\eta_j^2\eta_k^2$$

The constants c_1 , c_2 and A_1-A_7 are phenomenological parameters that can be fitted to reproduce the experimental phase diagram.

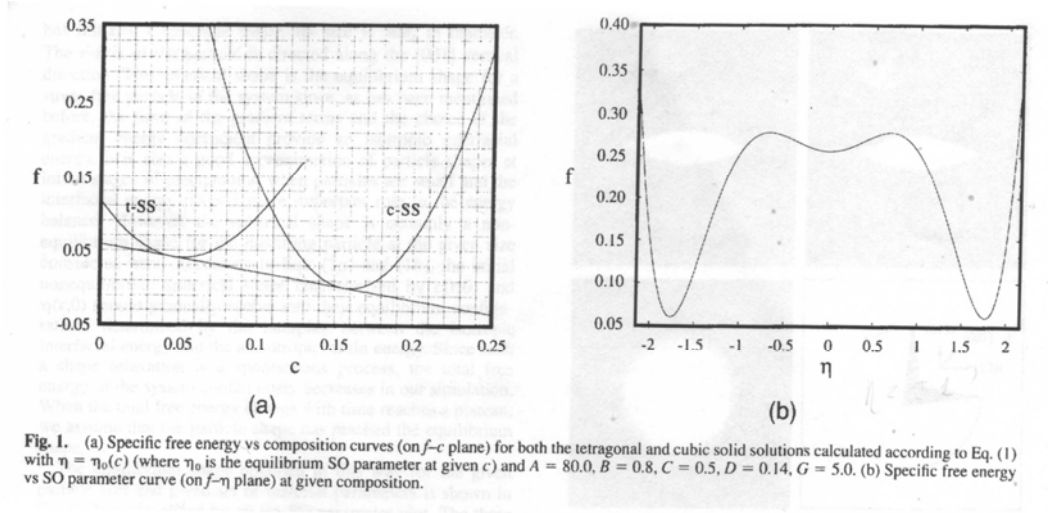

Fig. 1. (a) Specific free energy vs composition curves (on f–c plane) for both the tetragonal and cubic solid solutions calculated according to Eq. (1) with $\eta = \eta_0(c)$ (where η_0 is the equilibrium SO parameter at given c) and $A = 80.0$, $B = 0.8$, $C = 0.5$, $D = 0.14$, $G = 5.0$. (b) Specific free energy vs SO parameter curve (on f–η plane) at given composition.

From Y. Wang, L. Q. Chen and A. G. Khachaturyan: J . Am. Ceram. Soc. 79, p. 987, 1996.

Schematics illustrating the variations of $f(c,\eta_i)$ as a function of c and η_i.

✓Example 4: direct coupling with CALPHAD approach

(Shi et al, Acta Mat 2012)

Application to Ti-Al-V alloys

12 orientation variants

2 conserved order parameters Al and V

✓Free energy (Redlich-Kister polynomials) of each phase

$$G_m^{\alpha,\beta} = \sum_{i=Al,Ti,V} X_i \, {}^0G_i^{\alpha,\beta} + RT \sum_{i=Al,Ti,V} X_i \ln X_i + \sum_{i=Al,Ti,V} \sum_{j>i} \sum_{r=0}^{n} X_i X_j \left[{}^rL_{i,j}^{\alpha,\beta} \left(X_i - X_j \right)^r \right]$$

✓Interpolation to obtain a general expression of the free enrgy

$$G_m\left(T, X_k, \eta_i\right) = \sum_{i=1}^{12} h\left(\eta_i\right) G_m^{\alpha}\left(T, X_{Al,V}^{\alpha}\right) + \left(1 - \sum_{i=1}^{12} h\left(\eta_i\right)\right) G_m^{\beta}\left(T, X_{Al,V}^{\beta}\right) + \omega \sum_{i \neq j} \left|\eta_i \eta_j\right|$$

Interpolation functions $h\left(\eta_i\right) = \eta_i \left(6\eta_i^2 - 15\eta_i + 10\right)$

The gradient energy terms

$$\text{Gradient energy terms} = \int_{V_m}\int\int\left[\sum_{i=1}^{n}\frac{\alpha_i}{2}(\nabla c_i)^2 + \sum_{j=1}^{p}\frac{\beta_j}{2}(\nabla \eta_j)^2\right]dV$$

✓The gradient energy terms are associated to the interfacial energy, defined as the excess free energy associated with the compositional/structural inhomogeneities occuring at interfaces.

✓For the double-well potential, analytical relation between the interfacial energy γ and the stiffness parameter β:

$$\gamma = \frac{\Delta c^2 (A\beta/2)^{0.5}}{3}$$

✓For the other potentials, γ has to be evaluated numerically.

The long range energy contribution: the importance of the elastic energy

✓Particularly important since phase transformations in solids usually produces coherent microstructures at the early stages. The lattice mismatch between phases are accomodated by elastic displacements.

✓The elastic interactions play a major role in predicting the shape of the precipitates as well as the long range precipitates arrangements at the mesoscale.

✓Required ingredient to treat the microstructure of dislocations in phase field models.

…

Formation of chess-board like structure in Co-Pt alloys (from Le Bouar et al, acta mat, 1998)

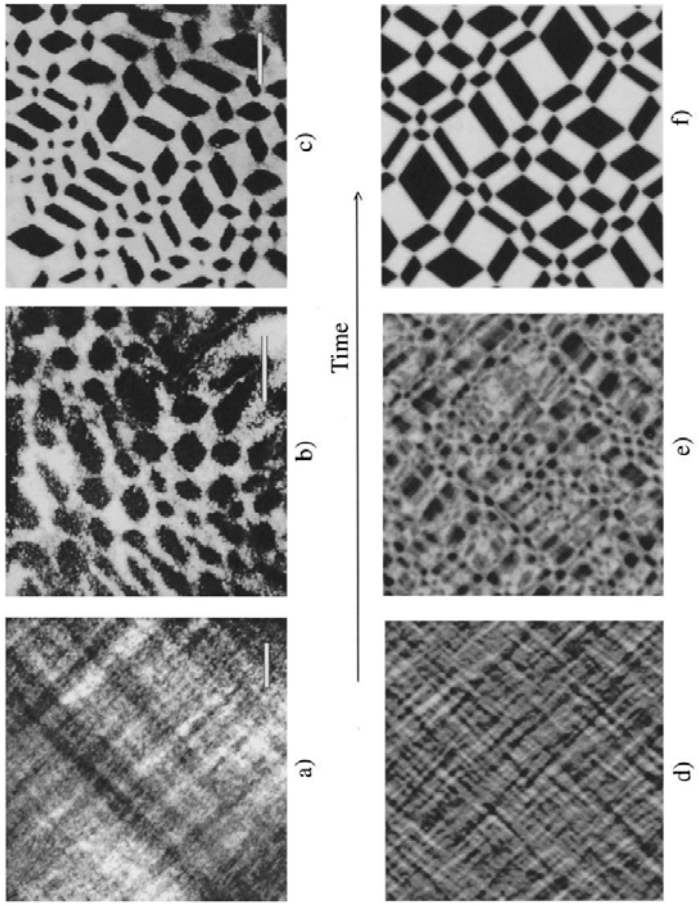

Growth of elastically strained thin films ($PbTiO_3$) on a substrate (from Li et al, App. Phys. Lett., 2001)

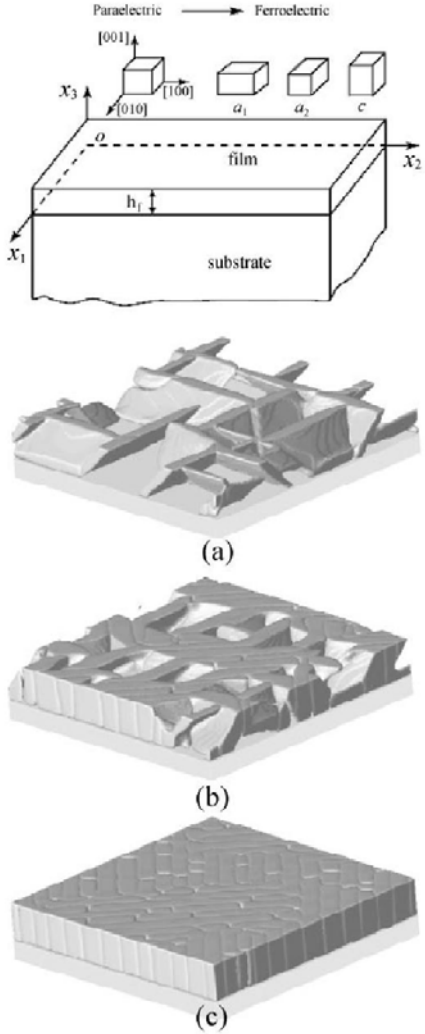

Elastic parameters

✓Elastic constants of the matrix: C^{m}_{ijkl}

✓Elastic constants of the precipitate: C^{p}_{ijkl}

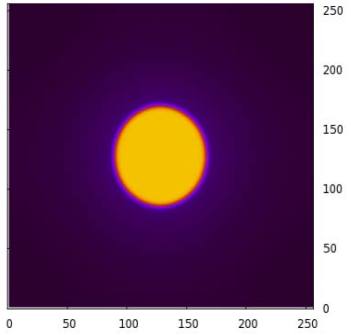

Voigt notation:

(i; i) → i, (2; 3) → 4, (1; 3) → 5, (1; 2) → 6

$$\begin{bmatrix} C_{11} & C_{12} & C_{12} & 0 & 0 & 0 \\ C_{12} & C_{11} & C_{12} & 0 & 0 & 0 \\ C_{12} & C_{12} & C_{11} & 0 & 0 & 0 \\ 0 & 0 & 0 & C_{44} & 0 & 0 \\ 0 & 0 & 0 & 0 & C_{44} & 0 \\ 0 & 0 & 0 & 0 & 0 & C_{44} \end{bmatrix}$$

Cubic systems

3 independent values:

C_{11}, C_{12}, C_{44}

$$\begin{bmatrix} C_{11} & C_{12} & C_{13} & 0 & 0 & 0 \\ C_{12} & C_{11} & C_{13} & 0 & 0 & 0 \\ C_{13} & C_{13} & C_{33} & 0 & 0 & 0 \\ 0 & 0 & 0 & C_{44} & 0 & 0 \\ 0 & 0 & 0 & 0 & C_{44} & 0 \\ 0 & 0 & 0 & 0 & 0 & \frac{C_{11}-C_{12}}{2} \end{bmatrix}$$

Hexagonal systems

5 independent values:

C_{11}, C_{33}, C_{12}, C_{13}, C_{44}

✓ Stress-free strain (STFS) associated to the transformation: ε_{ij}^{0}

To calculate the SFTS, it is required to choose 3 non collinear vectors in the matrix ($\mathbf{U_1}$, $\mathbf{U_2}$, $\mathbf{U_3}$) and to know their images after the transformation ($\mathbf{V_1}$, $\mathbf{V_2}$, $\mathbf{V_3}$), which allows to calculate the matrix transformation F:

$$\mathbf{V} = F\mathbf{U} \quad \Rightarrow \quad \varepsilon_{ij}^{0} = \frac{F^{t}F - I}{2}$$

✓Example 1: pure dilatation

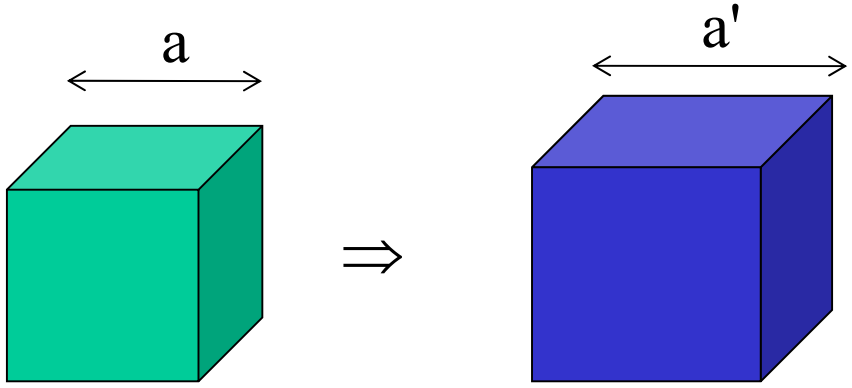

Cell of the matrix

Cell of the precipitate

$$\varepsilon_{ij}^{0} = \begin{bmatrix} \frac{a'-a}{a} & 0 & 0 \\ 0 & \frac{a'-a}{a} & 0 \\ 0 & 0 & \frac{a'-a}{a} \end{bmatrix}$$

✓Example 2: transformation of a hcp into fct phase, case of α→γ in zirconium alloys

Structure of α-Zr

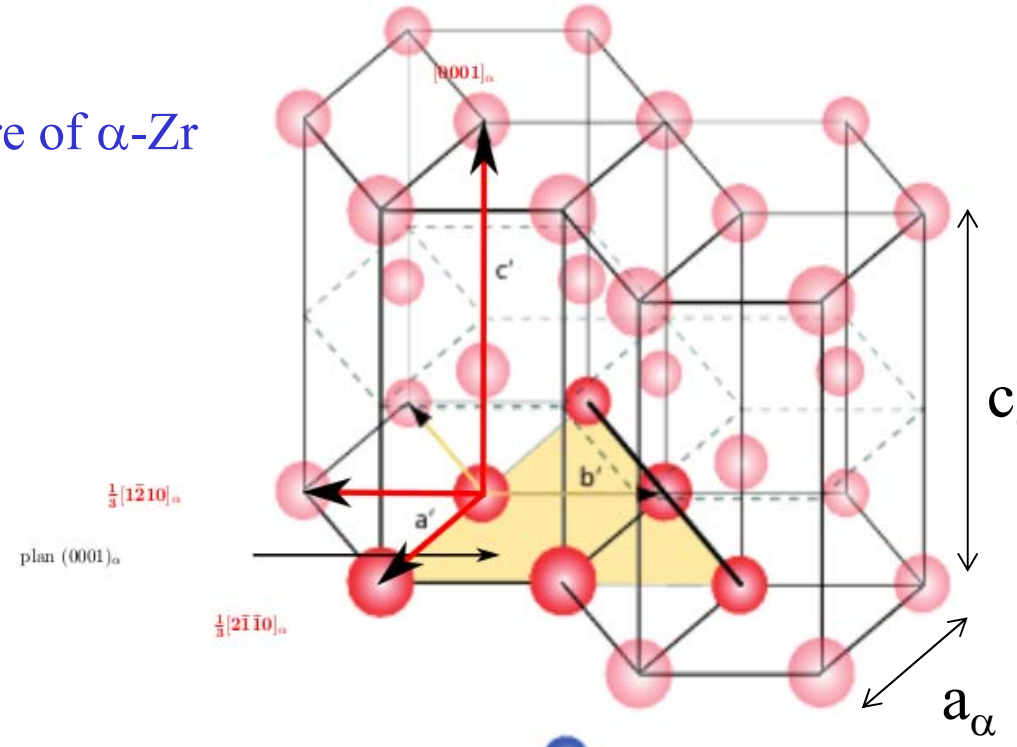

$$\varepsilon_{ij}^{0} = \begin{bmatrix} \varepsilon_{11}^{0} & 0 & 0 \\ 0 & \varepsilon_{22}^{0} & \varepsilon_{23}^{0} \\ 0 & \varepsilon_{23}^{0} & \varepsilon_{33}^{0} \end{bmatrix}_{(a,b,c)}$$

Structure of γ hydride

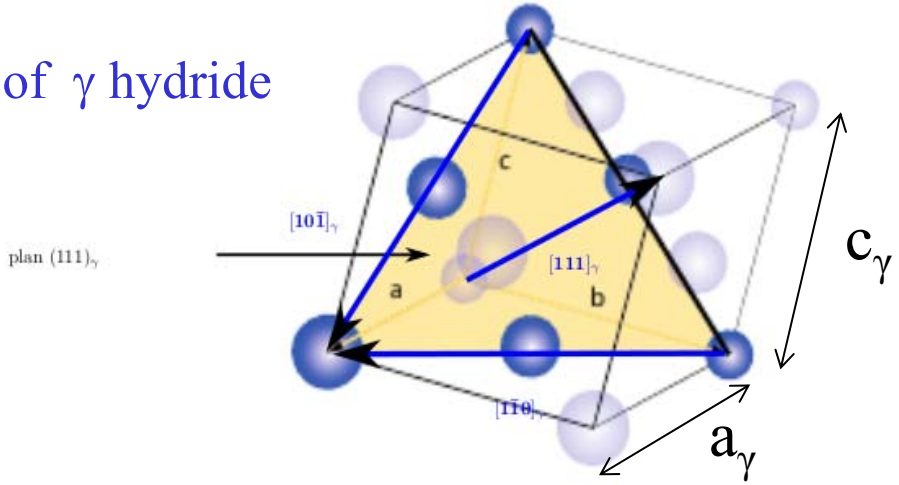

✓Each component depend on a_α, a_γ, c_α, and c_γ

How to calculate the elastic energy?

(Khachaturyan, *Theory of structural transformation in solids*, 1983)

✓Elastic energy: $$E_{elas} = \frac{1}{2}\int_V C_{ijkl}(\mathbf{r})\varepsilon^{el}_{ij}(\mathbf{r})\varepsilon^{el}_{kl}(\mathbf{r})dV$$

✓Total strain: $$\varepsilon_{ij}(\mathbf{r}) = \bar{\varepsilon}_{ij} + \delta\varepsilon_{ij}(\mathbf{r})$$

✓Elastic strain: $$\varepsilon^{el}_{ij}(\mathbf{r}) = \varepsilon_{ij}(\mathbf{r}) - \varepsilon^{0}_{ij}\theta(\mathbf{r})$$

($\theta(\mathbf{r}) = 1$ inside the precipitate, 0 inside the matrix
Order parameter of the phase-field model)

✓Elastic constants of the domain: $C_{ijkl}(\mathbf{r}) = C^{m}_{ijkl} + \Delta C_{ijkl}\theta(\mathbf{r})$, $\Delta C_{ijkl} = C^{p}_{ijkl} - C^{m}_{ijkl}$

✓Mechanical equilibrium: $$\frac{\partial \sigma_{ij}}{\partial r_j} = 0$$

$$\sigma_{ij}(\mathbf{r}) = C_{ijkl}(\mathbf{r})\varepsilon^{el}_{kl}(\mathbf{r})$$

$$\delta\varepsilon_{ij}(\mathbf{r}) = \frac{1}{2}\left(\frac{\partial u_i}{\partial r_j} + \frac{\partial u_j}{\partial r_i}\right)$$

1/ Homogeneous case: $C_{ijkl}(\mathbf{r}) = C^{m}_{ijkl} = C^{p}_{ijkl} = C_{ijkl}$

$$\Rightarrow \boxed{C_{ijkl}\frac{\partial^2}{\partial r_j \partial r_l}u_k(\mathbf{r}) = C_{ijkl}\varepsilon^0_{kl}\frac{\partial \Delta\theta(\mathbf{r})}{\partial r_j} = \sigma^0_{ij}\frac{\partial \Delta\theta(\mathbf{r})}{\partial r_j}}$$

Mechanical equilibrium in terms of displacements

✓Equation solved in the Fourier space (spectral method):

Discrete Fourier transform: $\theta(\mathbf{r}) = \sum_{\mathbf{K}} \theta(\mathbf{K})e^{i\mathbf{K}\mathbf{r}}$

Inverse Fourier transform: $\theta(\mathbf{K}) = \frac{1}{V}\int_V \theta(\mathbf{r})e^{-i\mathbf{K}\mathbf{r}}dV$

$V = L_1L_2L_3$

$L_i = N_i a_0$

a_0: grid spacing

Periodic boundary conditions: $K_i = 2\pi\frac{n_i}{L_i}$, $-N_i/2 < n_i \leq N_i/2$ $(n_i \in Z)$

$$TF\left(\frac{\partial f}{\partial r_i}\right) = ik_i TF(f)$$

$$C_{ijkl}\frac{\partial^2}{\partial r_j \partial r_l}u_k(\mathbf{r}) = C_{ijkl}\varepsilon^0_{kl}\frac{\partial \Delta\theta(\mathbf{r})}{\partial r_j} = \sigma^0_{ij}\frac{\partial \Delta\theta(\mathbf{r})}{\partial r_j} \Rightarrow -C_{ijkl}K_jK_lu_k(\mathbf{K}) = \sigma^0_{ij}(iK_j)\theta(\mathbf{K})$$

✓Linear system to inverse ($\mathbf{K}\neq\mathbf{0}$):

$$u_k(\mathbf{K}) = -i\Omega_{ki}\sigma^0_{ij}K_j\theta(\mathbf{K})$$

$$\Omega^{-1}_{ik} = C_{ijkl}n_jn_l$$

$$\mathbf{n} = \mathbf{K}/K$$

$$\Rightarrow \delta\varepsilon_{ij}(\mathbf{K})$$

For a fully relaxed simulation box $\quad \bar{\varepsilon}_{ij} = w_p\varepsilon^0_{ij}$

w_p : precipitate volume fraction

$$\Rightarrow E_{elas} = \frac{V}{2}\sum_{\mathbf{K}\neq\mathbf{0}} B(\mathbf{n})|\theta(\mathbf{K})|^2 \qquad B(\mathbf{n}) = \sigma^0_{ij}\varepsilon^0_{ij} - n_i\sigma^0_{ij}\Omega_{jm}(\mathbf{n})\sigma^0_{mn}n_n$$

2/ Heterogeneous case: $C^{m}_{ijkl} \neq C^{p}_{ijkl}$

$$[\bar{C}_{ijkl}\frac{\partial^2}{\partial r_j \partial r_l} + \underbrace{\Delta C_{ijkl}\frac{\partial}{\partial r_j}(\Delta\theta(\mathbf{r})\frac{\partial}{\partial r_l})}_{\text{Perturbation term}}]u_k(\mathbf{r}) = (C^{p}_{ijkl}\varepsilon^{0}_{kl} - \underbrace{\Delta C_{ijkl}\bar{\varepsilon}_{kl}}_{\text{Coupling with } \bar{\varepsilon}_{ij}})\frac{\partial \Delta\theta(\mathbf{r})}{\partial r_j}$$

$$\bar{C}_{ijkl} = w_p C^{p}_{ijkl} + (1 - w_p) C^{m}_{ijkl}$$

✓ Due to the perturbation term, no linear system in the Fourier space

$\Rightarrow$ Iterative procedure

(Khachaturyan et al, PRB 1995;
Hu and Chen, Acta mat 2001;
Boussinot et al, Acta Mat 2010;
Thuinet et al, Acta Mat 2012)

✓The displacement u is first initialized to the value u^0, which corresponds to the solution of the homogeneous system:

$$\bar{C}_{ijkl}\frac{\partial^2}{\partial r_j \partial r_l} u_k^0(\mathbf{r}) = C_{ijkl}^p \varepsilon_{kl}^0 \frac{\partial \Delta\theta(\mathbf{r})}{\partial r_j}$$

✓The solution is then determined iteratively using the following relation:

$$\bar{C}_{ijkl}\frac{\partial^2}{\partial r_j \partial r_l} u_k^{n+1}(\mathbf{r}) = (C_{ijkl}^p \varepsilon_{kl}^0 - \Delta C_{ijkl}\bar{\varepsilon}_{kl})\frac{\partial \Delta\theta(\mathbf{r})}{\partial r_j} + \Delta C_{ijkl}\frac{\partial}{\partial r_j}(\Delta\theta(\mathbf{r})\frac{\partial}{\partial r_l})u_k^n(\mathbf{r})$$

✓In the Fourier space:

$$\Rightarrow \quad u_k^{n+1}(\mathbf{K}) = -i\Omega_{ki}\left[(C_{ijkl}^p \varepsilon_{kl}^0 - \Delta C_{ijkl}\bar{\varepsilon}_{kl})K_j\theta(\mathbf{K}) + \Delta C_{ijkl}\mathrm{TF}\{\frac{\partial}{\partial r_j}(\Delta\theta(\mathbf{r})\frac{\partial}{\partial r_l})u_k^n(\mathbf{r})\}\right]$$

$$\Omega_{ik}^{-1} = \bar{C}_{ijkl}n_j n_l$$

✓Practically, the number of iterations depends on ΔC_{ijkl}

✓Case of an applied stress:

$$\bar{\varepsilon}_{ij} = \underbrace{w_p \varepsilon^0_{ij}}_{\text{transformation}} + \underbrace{\bar{S}_{ijkl}\sigma^a_{kl}}_{\text{applied stress}}$$

σ^a_{kl} : applied stress

$\bar{S}_{ijkl}$: compliance tensor

✓Example: Study of a trigonal perturbation C_{15} inside a precipitate

Elastic trigonal perturbation inside the precipitate

homogeneous isotropic domain

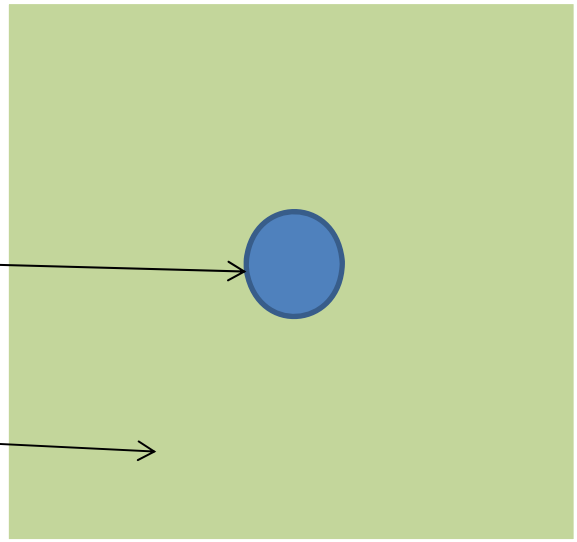

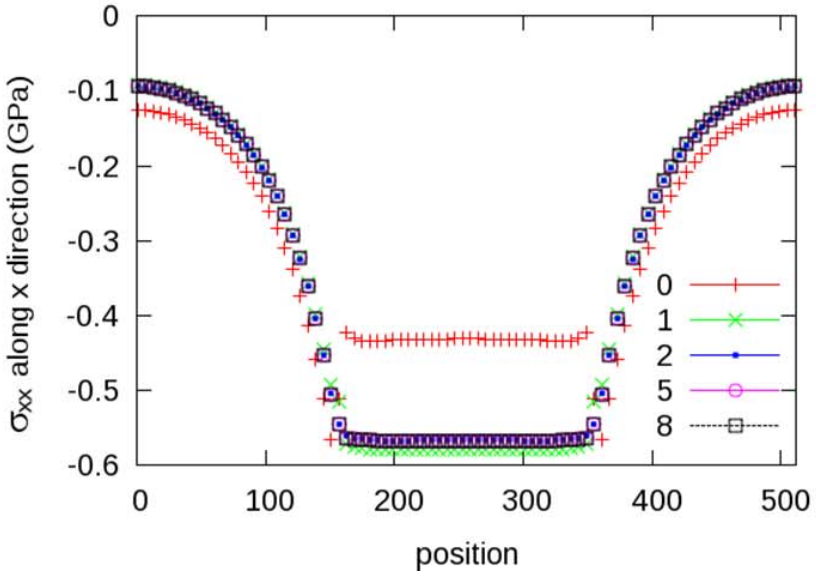

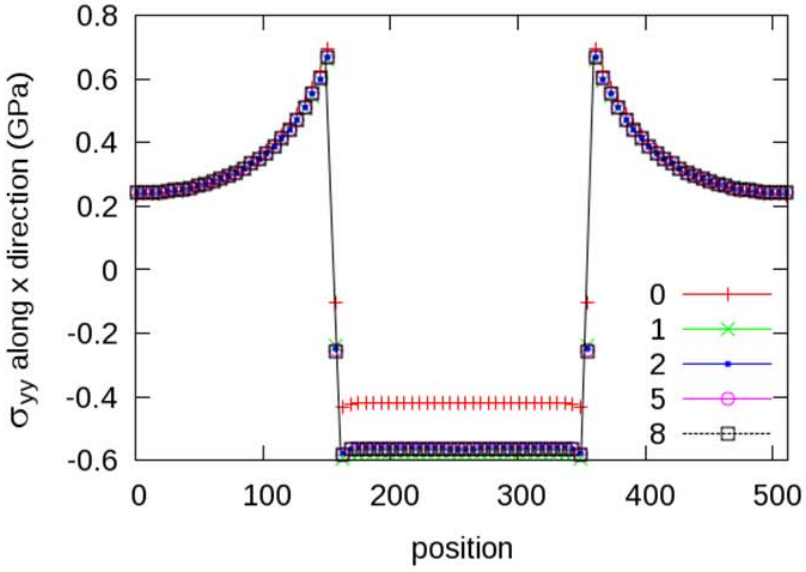

(From Thuinet et al, Acta Mat 2012)

Which morphology minimizes the elastic energy? (homogeneous elasticity)

$$E_{elas} = \frac{V}{2} \sum_{K \neq 0} B(\mathbf{n}) |\theta(\mathbf{K})|^2$$

Elastic parameters Microstructure

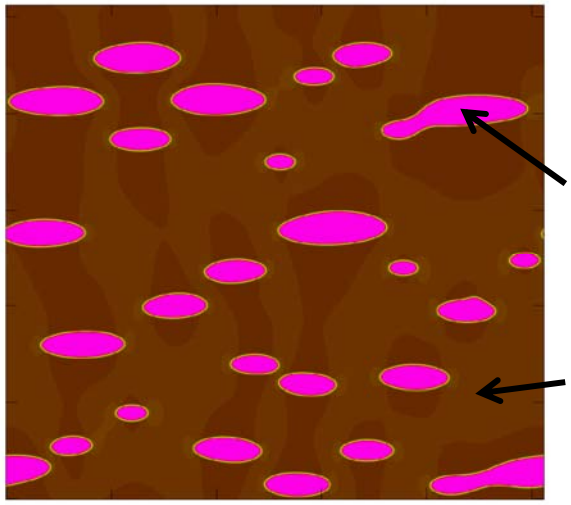

$$B(\mathbf{n}) = \sigma^0_{ij}\varepsilon^0_{ij} - n_i\sigma^0_{ij}\Omega_{jm}(\mathbf{n})\sigma^0_{mn}n_n$$

C_{ijkl}, ε^0_{ij}

$$E_{elas} \geq \frac{V}{2} \min_{\mathbf{n}} B(\mathbf{n}) \sum_{K \neq 0} |\theta(\mathbf{K})|^2$$

$$\Rightarrow \quad E_{elas} \geq \frac{V_p}{2} \min_{\mathbf{n}} B(\mathbf{n})$$

Parseval theorem $|\theta(\mathbf{K})|^2 = \frac{V_p}{V}$

$\min_{\mathbf{n}} B(\mathbf{n}) = B(\mathbf{n_0})$ $\quad\quad$ $\mathbf{n_0}$ is the direction which minimizes $B(\mathbf{n})$

$\theta(\mathbf{K}) = 0$ if $\mathbf{K}/K \neq \mathbf{n_0}$

$$\Rightarrow \quad E_{elas} = \frac{V}{2}\sum_{K\neq 0} B(\mathbf{n})|\theta(\mathbf{K})|^2 = \frac{V}{2} B(\mathbf{n_0}) \sum_{K\neq 0} |\theta(\mathbf{K})|^2 = \frac{V_p}{2} B(\mathbf{n_0})$$

✓The morphology which minimizes the elastic energy is a platelet the normal of which is $\mathbf{n_0}$

✓n_0 also called the elastically soft directions

✓Application to the determination of the habit plane or facetting of precipitates

Example 1: cubic system, isotropic SFTS tensor

$2C_{44} + C_{11} - C_{12} > 0 \Rightarrow \mathbf{n_0} = \langle 100 \rangle$

$2C_{44} + C_{11} - C_{12} < 0 \Rightarrow \mathbf{n_0} = \langle 111 \rangle$

(J.W. Cahn, Acta Metall., 1962)

Example 2: hexagonal system, isotropic SFTS tensor

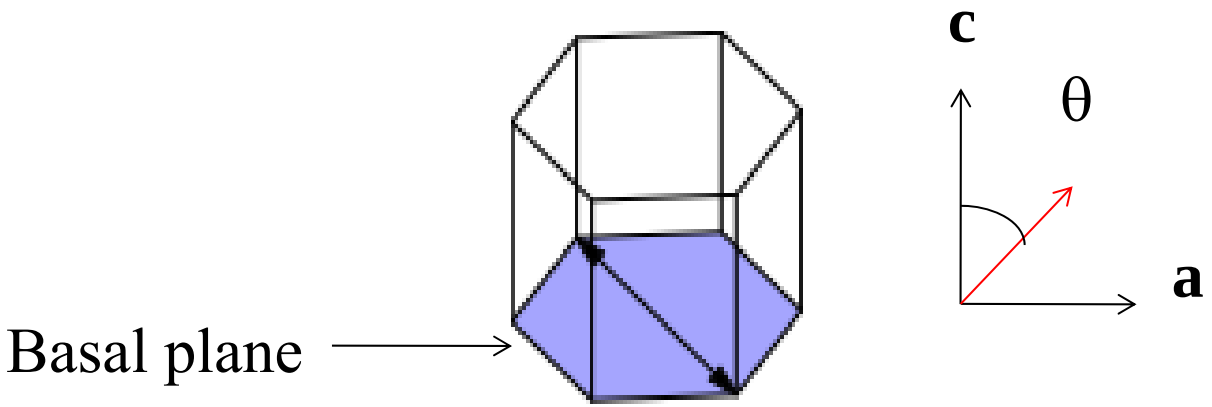

✓5 independent elastic constants C_{11}, C_{33}, C_{12}, C_{13}, C_{44}

✓Isotropic in the basal plane

✓Classification which depends on 2 threshold values for C_{44}:

$$[C_{44}]_{th1} = \frac{1}{2}\frac{C_{11}C_{33} + C_{12}C_{33} - 2C_{13}^2}{C_{33} + 2C_{13}} \qquad [C_{44}]_{th2} = \frac{1}{2}\frac{C_{11}C_{13} - C_{12}C_{13} + C_{11}C_{33} - C_{13}^2}{C_{11} + C_{12} + C_{13}}$$

✓ First case: $[C_{44}]_{th1} < [C_{44}]_{th2}$

- $C_{44} < [C_{44}]_{th1}$ $\quad \theta_s = \theta_0 \quad \theta_h = 90°$
- $[C_{44}]_{th1} < C_{44} < [C_{44}]_{th2}$ $\quad \theta_s = 0° \quad \theta_h = 90°$
- $[C_{44}]_{th2} < C_{44}$ $\quad \theta_s = 0° \quad \theta_h = \theta_0$

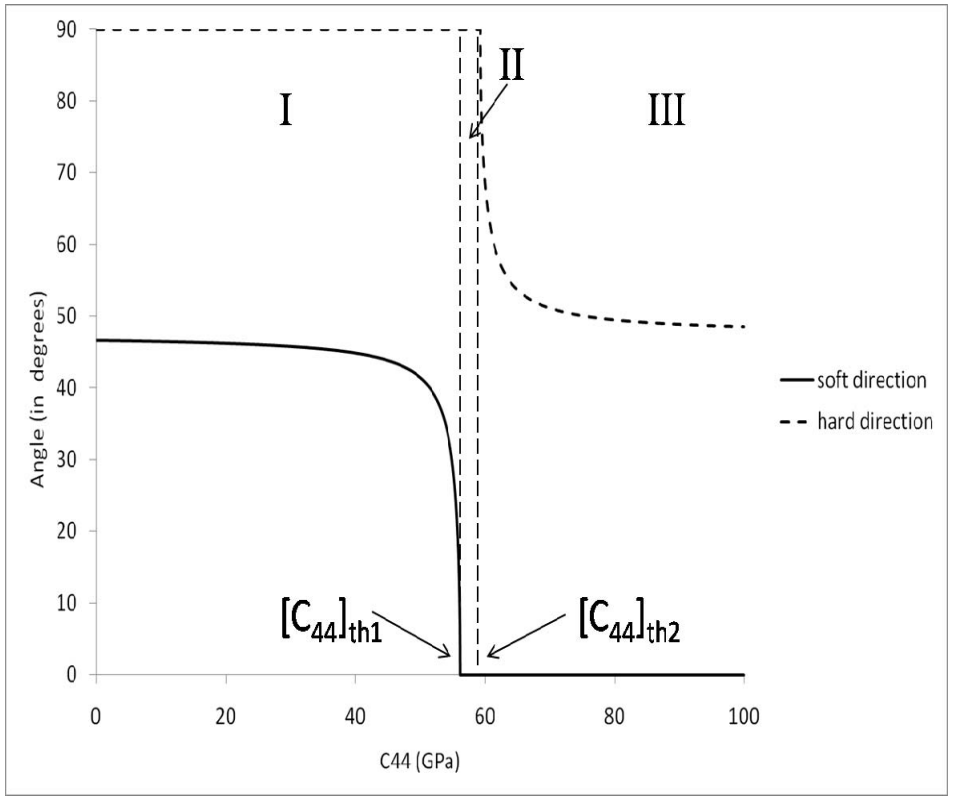

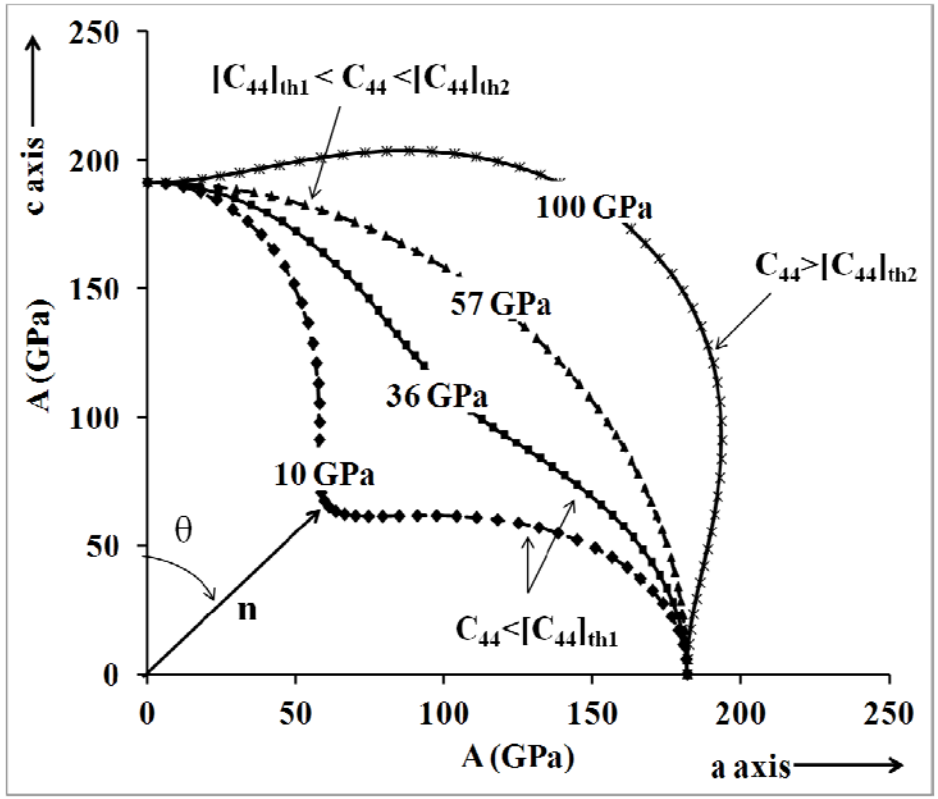

$$\theta_0 = \frac{1}{2}\cos^{-1}\left(-\frac{I}{J}\right)$$

with I and J functions of the elastic constants:

$I = - C_{12}C_{13} + (C_{13})^2 - C_{12}C_{33} + C_{11}(C_{13}-2C_{44}) - 2C_{12}C_{44} + 2C_{13}C_{44} + 2C_{33}C_{44}$

$J = 3(C_{13})^2 - C_{11}(C_{13} + 2C_{33} - 2C_{44}) + 6C_{13}C_{44} + 2C_{33}C_{44} + C_{12}(C_{13} - C_{33} + 2C_{44})$

✓Second case: $[C_{44}]_{th2} < [C_{44}]_{th1}$

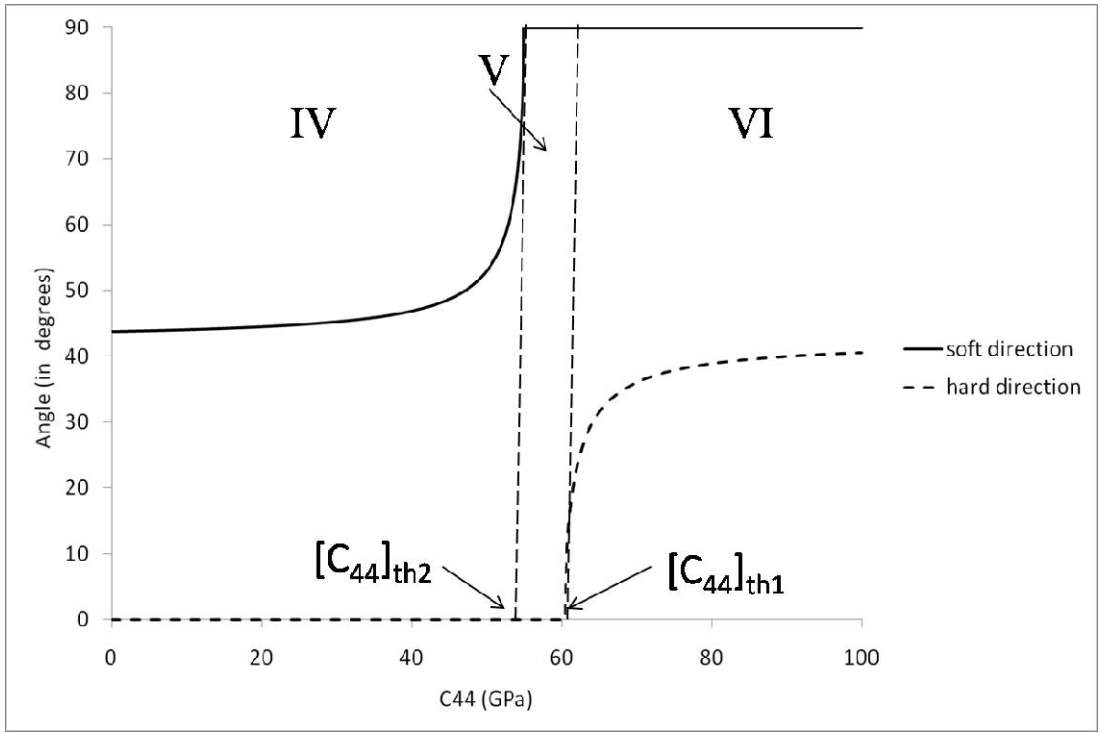

Classification of hexagonal systems

Family	Criterion	θ_s	θ_h
I	$[C_{44}]_{th2} > [C_{44}]_{th1} > C_{44}$	θ_0	90°
II	$[C_{44}]_{th1} < C_{44} < [C_{44}]_{th2}$	0	90°
III	$C_{44} > [C_{44}]_{th2} > [C_{44}]_{th1}$	0	θ_0
IV	$[C_{44}]_{th1} > [C_{44}]_{th2} > C_{44}$	θ_0	0
V	$[C_{44}]_{th2} < C_{44} < [C_{44}]_{th1}$	90°	0
VI	$C_{44} > [C_{44}]_{th1} > [C_{44}]_{th2}$	90°	θ_0

(From Thuinet et al, APL 2012)

✓In the case of homogeneous or heterogeneous elasticity, the elastic energy can be easily evaluated for any arbitrary microstructures in the Fourier space.

✓In fact, the notion of SFTS can be applied to a large diversity of cases

✓Example 1: homogeneous solid solution

this formalism has been extended in the framework of the microscopic elasticity theory of homogeneous solid solutions to take into account long range elastic interaction between the different species diffusing inside a solid solution.

Coherent Inclusion Model | Solid Solution Model (long-wave limit)

(Khachaturyan, *Theory of structural transformation in solids*, 1983)

$\theta_p(r,t)$: shape function of precipitate of type p

$c_p(r,t)$: composition of species p

$$E_{elas} = \frac{V_m}{2} \sum_{k \neq 0} \sum_{p,q} B_{pq}(\vec{k}) \theta_p(\vec{k}) \theta_q^*(\vec{k})$$

$$B_{pq}(\vec{k}) = \sigma_{ij}^{00}(p) \varepsilon_{ij}^{00}(q) - k_i \sigma_{ij}^{00}(p) G_{jm}(\vec{k}) \sigma_{mn}^{00}(q) k_n$$

$$E_{elas} = \frac{V_m}{2} \sum_{k \neq 0} \sum_{p,q} B_{pq}(\vec{k}) c_p(\vec{k}) c_q^*(\vec{k})$$

$$B_{pq}(\vec{k}) = \sigma_{ij}^{00}(p) u_{ij}^{00}(q) - k_i \sigma_{ij}^{00}(p) G_{jm}(\vec{k}) \sigma_{mn}^{00}(q) k_n$$

$G_{ij}(k)=(\lambda_{ijkl} k_m k_l)^{-1}$ Fourier transform of the Green function

$$\sigma_{ij}^{00}(p) = \lambda_{ijkl} \varepsilon_{kl}^{00}(p)$$

$\varepsilon_{kl}^{00}(p)$: stress free strain

$$\sigma_{ij}^{00}(p) = \lambda_{ijkl} u_{kl}^{00}(p)$$

$u_{kl}^{00}(p)$: linear expansion coefficient related to alloying (Vegard's Law)

✓Example 2: dislocations

According to the result of Nabarro (Theory of crystal dislocations, 1967), one dislocation loop is elastically equivalent to a platelet of thickness d it encompasses and characterized by a SFTS defined as:

$$\varepsilon_{ij}^{\eta} = \frac{1}{2d}(b_i n_j + b_j n_i)$$

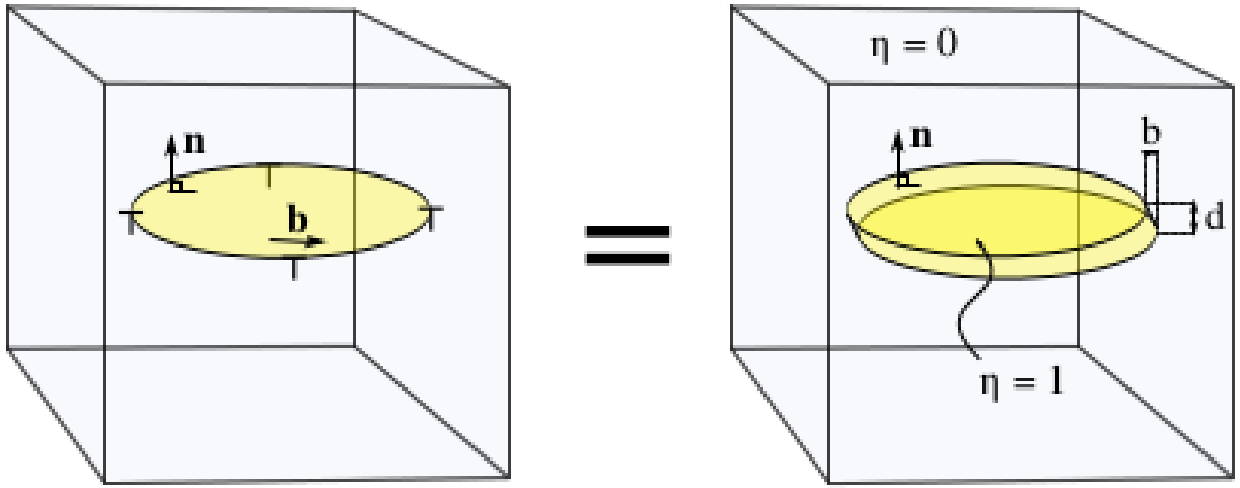

(Wang et al, Acta Mater. 49, 2001
Rodney et al, Acta Mater. 51, 2003)

✓Example 3: crystalline plasticity

Individual treatment of each dislocation may be computationally prohibitive at mesoscale

⇒Use of crystalline plasticity model to calculate the plastic strain

$$E_{elas} = \frac{1}{2}\iiint \lambda_{ijkl}(r)\left(\varepsilon_{ij}(r) - \varepsilon^0_{ij}(r) - \varepsilon^p_{ij}(r)\right)\left(\varepsilon_{ij}(r) - \varepsilon^0_{ij}(r) - \varepsilon^p_{ij}(r)\right)dV - V_m \sigma^a_{ij}\bar{\varepsilon}_{ij}$$

The plastic strain can be numerically treated in the same way as any SFTS for the calculation of the displacement field. For example, in the case of homogeneous elasticity:

$$u_k(\mathbf{K}) = -i\Omega_{ki}C_{ijkl}K_j\left[\varepsilon^0_{kl}\theta(\mathbf{K}) + \varepsilon^p_{kl}(\mathbf{K})\right]$$

Phase transformation **Plastic effect**

Crystalline plasticity model:

- *Plastic strain :* $\dot{\varepsilon}^{p}_{ij} = \sum R^{r}_{ij}\dot{\gamma}^{r}$ **r : slip system**
- *Shear rate :* $\dot{\gamma}^{r} = \rho^{r} b^{r} v^{r}$ *dislocations velocity :* $v^{r} = v^{r}_{0}\exp\left(\frac{-\mu(b^{r})^{3}}{2k_{b}T}\right)\left[\frac{|\tau^{r}| - \tau^{r}_{c}}{\tau^{r}_{cut}}\right]^{n}$
- *Density dislocations evolution law :*

$$\dot{\rho}^{r} = \left(\frac{1}{L^{r}} - 2y^{r}_{c}\rho^{r}\right)\frac{|\dot{\gamma}^{r}|}{b^{r}} \quad \text{with} \quad L^{r} = K_{L}\Big/\sqrt{\left(\sum a^{rh}\rho^{h}\right)}$$

- *Plastic activation:*

$$\tau^{r} = R^{r} : \sigma \quad > \quad \tau^{r}_{c} = \tau^{r}_{c0} + \mu b^{r}\sqrt{\left(\sum a^{rh}\rho^{h}\right)}$$

(Kundin et al, Journal of the Mechanics and Physics of Solids 59, 2011
Kundin et al, Journal of the Mechanics and Physics of Solids 76, 2015)

Kinetics

✓ How to deal with kinetics?

In the general case, little is known about the time evolution of a system being held far from the thermodynamic equilibrium. However, the thermodynamics of irreversible processes (TIP) in the linear response approximation has been proven to successfully describe a great variety of situations. In this framework a distinction is made between conserved and non conserved order parameters:

$$\frac{\partial \eta_p(\mathbf{r},t)}{\partial t} = -L_p \nabla \frac{\delta F}{\delta \eta_p(\mathbf{r},t)}$$

for the non conserved order parameters
(Allen-Cahn or Ginzburg-Landau equation)

$$\frac{\partial c(\mathbf{r},t)}{\partial t} = M \nabla^2 \frac{\delta F}{\delta c(\mathbf{r},t)}$$

for the conserved order parameters
(Cahn-Hilliard equation)

The knowledge of the free energy and the kinetic coefficients provides a consistent set for the calculation of the microstructure time evolution.

Application to irradiation:

✓The Cahn-Hilliard equation can incorporate supplementary terms to take into account generation of defects due to irradiation and recombination

✓Example: conservation equation for vacancies

$$\frac{\partial c_v(r,t)}{\partial t} = M\nabla^2 \frac{\delta F}{\delta c_v} + \underbrace{\dot{g}(c_v(r,t))}_{\text{Production term}} - \underbrace{\dot{\gamma}(c_v(r,t), c_{SIA}(r,t))}_{\text{Recombination term}}$$

✓Example: resolution of the kinetic equation with the semi-implicit spectral method

✓One order parameter $c(\mathbf{r},t)$

✓Cahn-Hilliard equation $$\frac{\partial c(\mathbf{r},t)}{\partial t} = M\nabla^2 \frac{\delta F}{\delta c(\mathbf{r},t)} \qquad F=F_{chem}+E_{elas}$$

✓Short-range contribution $$F_{chem} = \int_{V_m}\int\int [f_{hom}(c) + \frac{\beta}{2}(\nabla c)^2]dV$$

✓Long-range contribution (homogeneous elasticity) $$E_{elas} = \frac{V_m}{2}\sum_{\kappa} B(\mathbf{n})c(\mathbf{K})c^*(\mathbf{K})$$

✓Functional derivatives:

$$\frac{\delta}{\delta c}\int_{V_m}\int\int f_{hom}(c)dV = \frac{\partial f_{hom}}{\partial c}$$

$$\frac{\delta}{\delta c}\int_{V_m}\int\int \frac{\beta}{2}(\nabla c)^2 dV = -\beta\nabla^2 c$$

✓Spectral method:

$$\frac{\partial c(\mathbf{K})}{\partial t} = -MK^2\left[\frac{\partial f_{hom}}{\partial c}(\mathbf{K}) + \beta K^2 c(\mathbf{K}) + \frac{\delta E_{elas}}{\delta c}(\mathbf{K})\right]$$

✓Explicit temporal discretization:

$$c(\mathbf{K},t+dt) = c(\mathbf{K},t) - MK^2 dt\left[\frac{\partial f_{hom}}{\partial c}(\mathbf{K},t) + \beta K^2 c(\mathbf{K},t) + \frac{\delta E_{elas}}{\delta c}(\mathbf{K},t)\right]$$

✓Implicit temporal discretization:

$$c(\mathbf{K},t+dt) = c(\mathbf{K},t) - MK^2 dt\left[\frac{\partial f_{hom}}{\partial c}(\mathbf{K},t+dt) + \beta K^2 c(\mathbf{K},t+dt) + \frac{\delta E_{elas}}{\delta c}(\mathbf{K},t+dt)\right]$$

✓Semi-implicit temporal discretization:

$$c(\mathbf{K},t+dt) = c(\mathbf{K},t) - MK^2 dt\left[\frac{\partial f_{hom}}{\partial c}(\mathbf{K},t) + \beta K^2 c(\mathbf{K},t+dt) + \frac{\delta E_{elas}}{\delta c}(\mathbf{K},t)\right]$$

$$\Rightarrow \quad c(\mathbf{K},t+dt) = \frac{c(\mathbf{K},t) - MK^2 dt\left[\frac{\partial f_{hom}}{\partial c}(\mathbf{K},t) + \frac{\delta E_{elas}}{\delta c}(\mathbf{K},t)\right]}{1+M\beta K^4 dt}$$

✓Advantage of the spectral method: simple form of the elastic driving force

$$\frac{\delta E_{elas}}{\delta c}(\mathbf{K},t) = B(\mathbf{K})c(\mathbf{K})$$

✓Advantage of the semi-implicit method: simplicity of the explicit scheme but use of larger numerical time steps

(Chen & Shen, J. Comput. Phys. Commun. 1998)

Advantages

✓Time and space scale ‘meso’ in general above those spanned by atomic scale modelling

✓Presence of space (in contrast with Rate Theory, for example)

✓Long-range effects naturally included

Limitations

✓Time and space scale ‘meso’ in general too high to treat nucleation

✓Time and space scale ‘meso’ in general too small to treat macroscopic problems: a good coupling with macro models must be elaborated

Application 1:

Morphological bifurcation

✓Morphology of the precipitate controlled by the competition between the interfacial energy and the elastic energy

✓Morphology which minimizes the interfacial contribution (isotropic interfacial energy): sphere

✓Morphology which minimizes the elastic energy: platelet

✓The interfacial energy is proportional to the interfacial surface

✓The elastic energy is proportional to the volume

Example: transition between square and plaquette

$$L = \frac{\varepsilon^2 C_{44} r_p}{\gamma} > 5.6$$

(Thompson et al, Acta Metall Mater 1994;42)

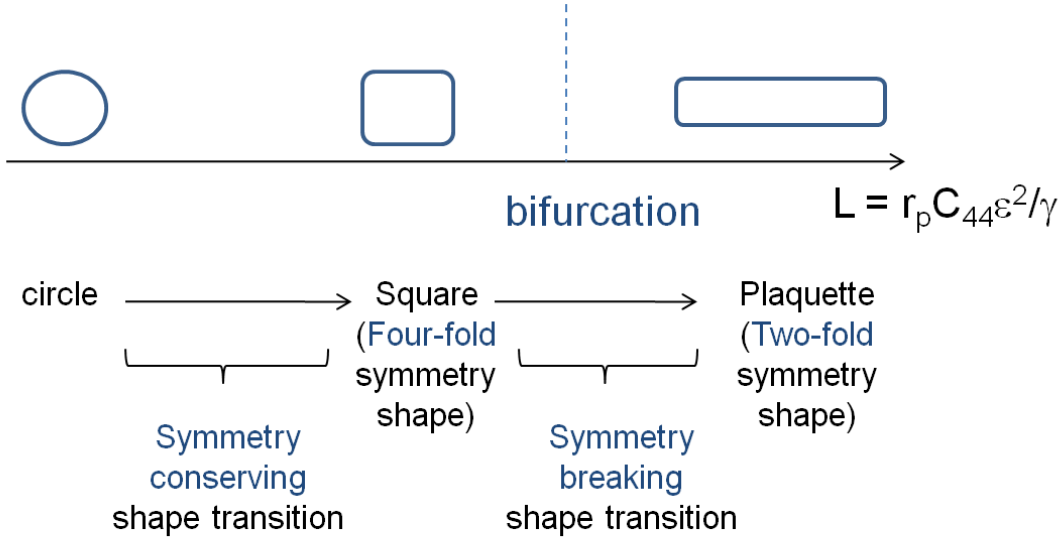

b) Homogeneous cubic system

Problem

Symmetry break between α matrix (hexagonal cristalline system) and ζ precipitate (trigonal cristalline system)

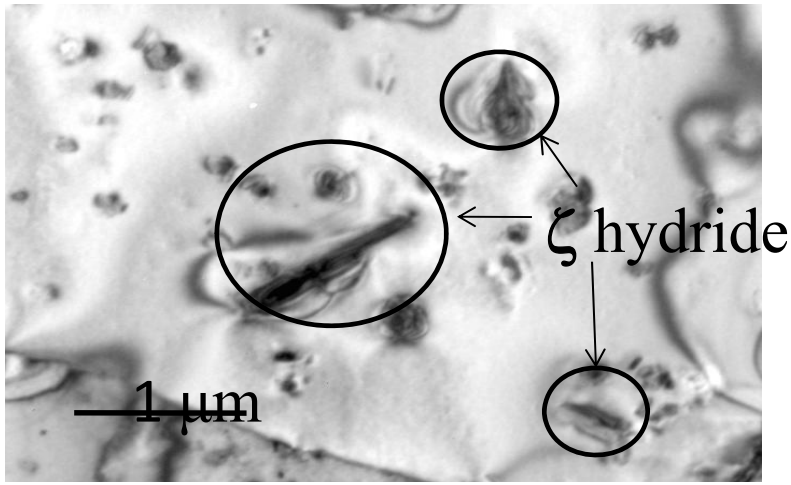

Fig. TEM Micrograph of intragranular ζ hydrides inside the basal plane of the hexagonal matrix

⊙ [0001]

3 orientation variants: precipitates aligned with dense directions < -1-1 2 0> inside the basal plane of the hexagonal matrix

Influence of the symmetry break on:

- The elastic properties of the system
- The resulting morphology of the coherent hydrides

New ζ hydride phase identification

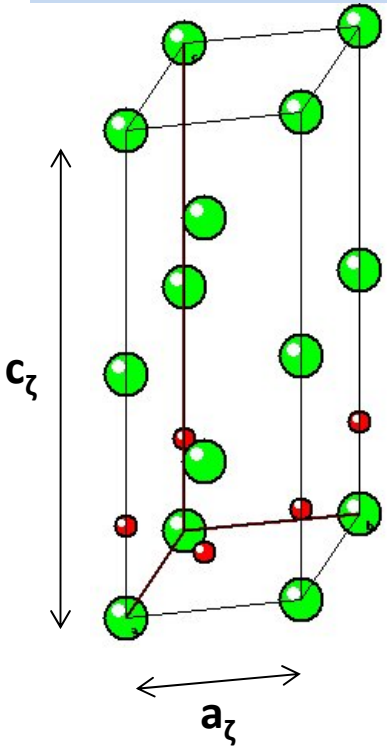

Coherent hydride with the matrix
Needle-like morphology
Length: 100-500nm

4 Zr atoms

2 H atoms

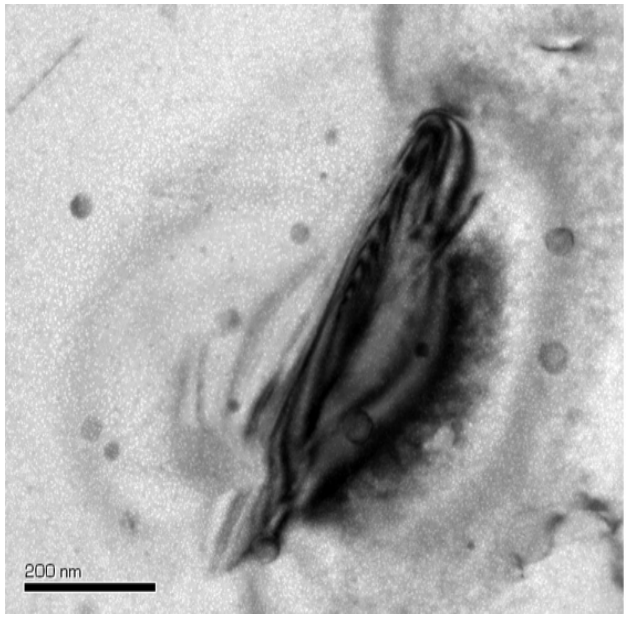

TEM micrograph of ζ hydride

Z. Zhao, J.-P. Morniroli, A. Legris, A. Ambard, Y. Khin, L. Legras & M. Blat-Yrieix, "Identification and characterization of a new zirconium hydride", Journal of Microscopy, Vol. 232, 2008, pp. 410-421

- Cristalline system : TRIGONAL
- Bravais lattice: HEXAGONAL

  $a_\zeta = a_{Zr\alpha} = 3.232$ Å

  $c_\zeta = 2c_{Zr\alpha} = 10.294$ Å

- Space group : 3Pm1
- Stoechiometry : Zr_2H
- Metastable phase

Stress-free strain

Stress-free strain tensor associated with $\alpha \rightarrow \zeta$ transformation must respect the symmetry elements of both matrix and precipitate, i.e. must be invariant by $2\pi/3$ rotation around **c** axis (//[0001])

$$\Rightarrow \boldsymbol{\varepsilon}_{ij}^{0}(\alpha \rightarrow \zeta) = \begin{bmatrix} \varepsilon_{11}^{0} & 0 & 0 \\ 0 & \varepsilon_{11}^{0} & 0 \\ 0 & 0 & \varepsilon_{33}^{0} \end{bmatrix}_{([10\bar{1}0],[\bar{1}2\bar{1}0],[0001])}$$

- Transversely isotropic tensor in the basal plane
- The same stress-free strain tensor is associated to each orientation variant

Elastic constants

⇒ 5 independant elastic constants in the hexagonal matrix

⇒ 1 supplementary elastic constant in the trigonal precipitate (c_{15})

phase	Matrix α	Precipitate ζ
Point group	6/mmm (hexagonal)	3m1 (trigonal)
Voigt constants matrix	$\begin{bmatrix} c_{11} & c_{12} & c_{13} & 0 & 0 & 0 \\ c_{12} & c_{11} & c_{13} & 0 & 0 & 0 \\ c_{13} & c_{13} & c_{33} & 0 & 0 & 0 \\ 0 & 0 & 0 & c_{44} & 0 & 0 \\ 0 & 0 & 0 & 0 & c_{44} & 0 \\ 0 & 0 & 0 & 0 & 0 & \frac{c_{11}-c_{12}}{2} \end{bmatrix}$	$\begin{bmatrix} c_{11} & c_{12} & c_{13} & 0 & c_{15} & 0 \\ c_{12} & c_{11} & c_{13} & 0 & -c_{15} & 0 \\ c_{13} & c_{13} & c_{33} & 0 & 0 & 0 \\ 0 & 0 & 0 & c_{44} & 0 & -c_{15} \\ c_{15} & -c_{15} & 0 & 0 & c_{44} & 0 \\ 0 & 0 & 0 & -c_{15} & 0 & \frac{c_{11}-c_{12}}{2} \end{bmatrix}$
Numerical values (in GPa)	c_{11}=155; c_{12}=67; c_{13}=65; c_{33}=173; c_{44}=36 (experimental values, Fast et al., *Phys. Rev. B*, 1995)	c_{11}=168; c_{12}=89; c_{13}=67; c_{33}=195; c_{44}=29; c_{15}=-23 (experimental values, Fast et al., *Phys. Rev. B*, 1995 + ab initio calculations)

Phase field simulations

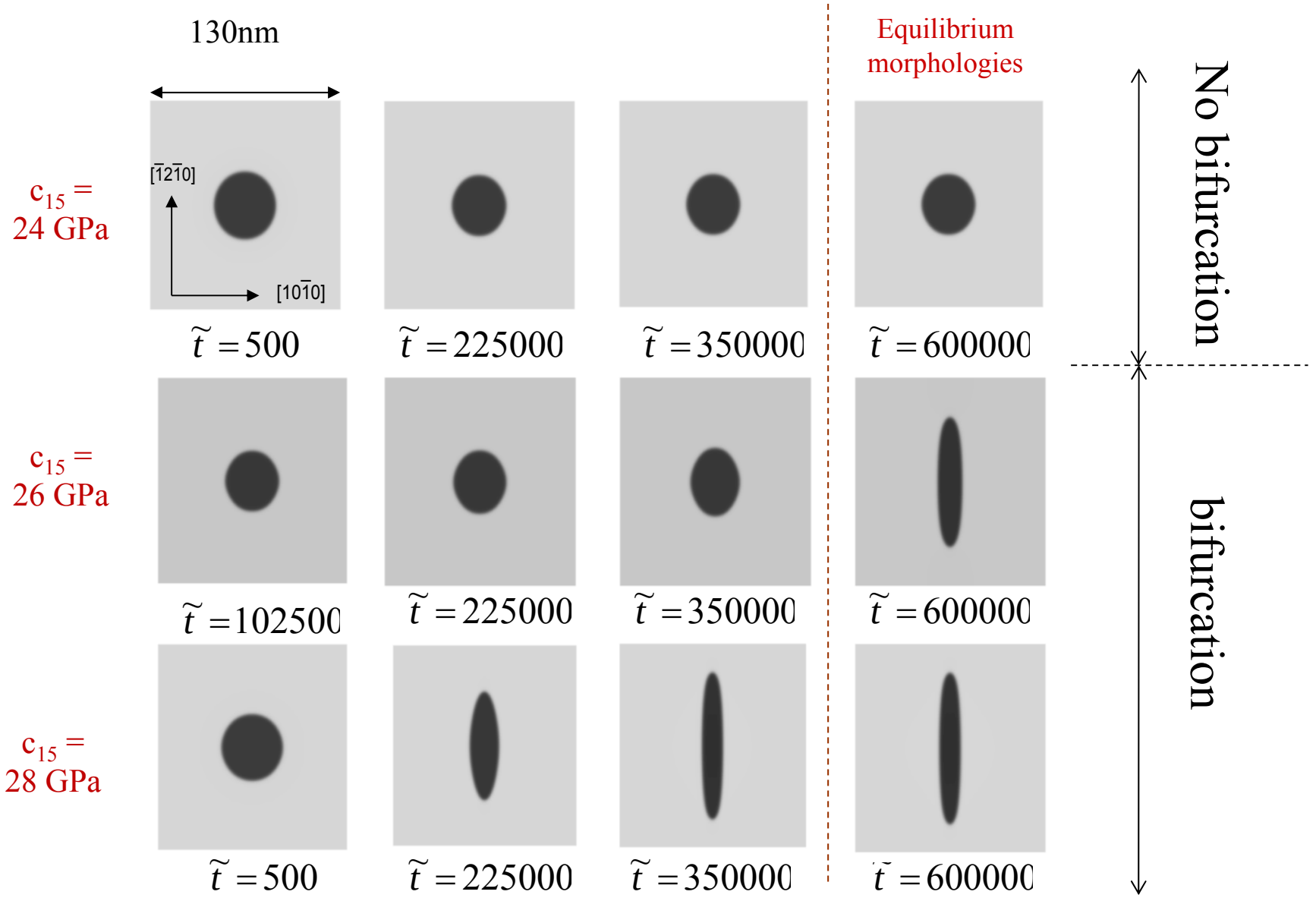

(Thuinet et al, Acta Mat 2012)

Influence of direction and magnitude of stress on the re-orientation kinetics of hydrides in the basal plane

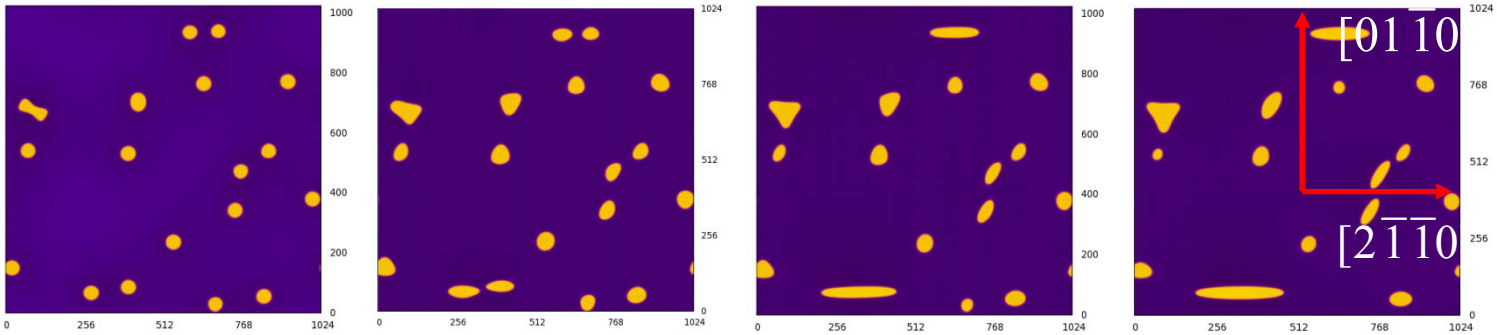

Applied Stress

τ=5000 τ=50k τ=100k τ=150k

0MPa

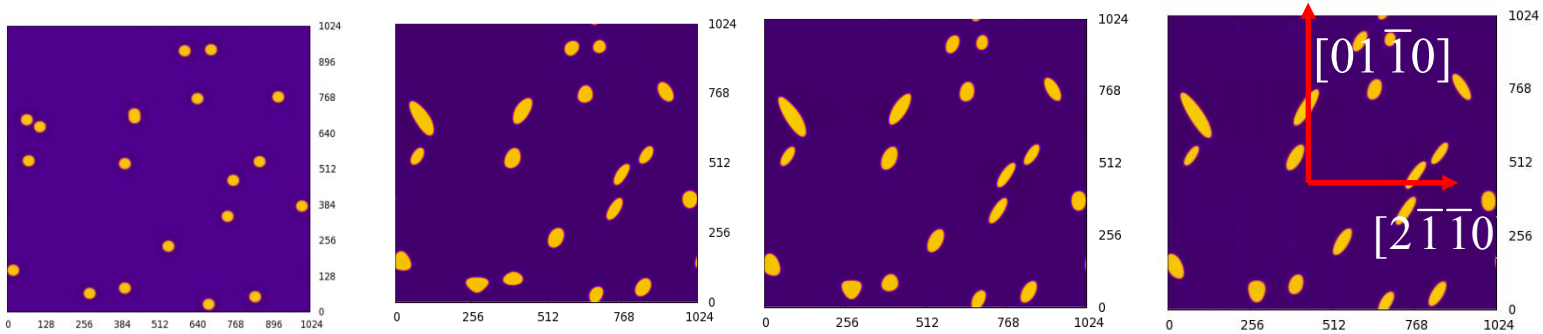

τ=1 τ=10k τ=20k τ=35k

300MPa

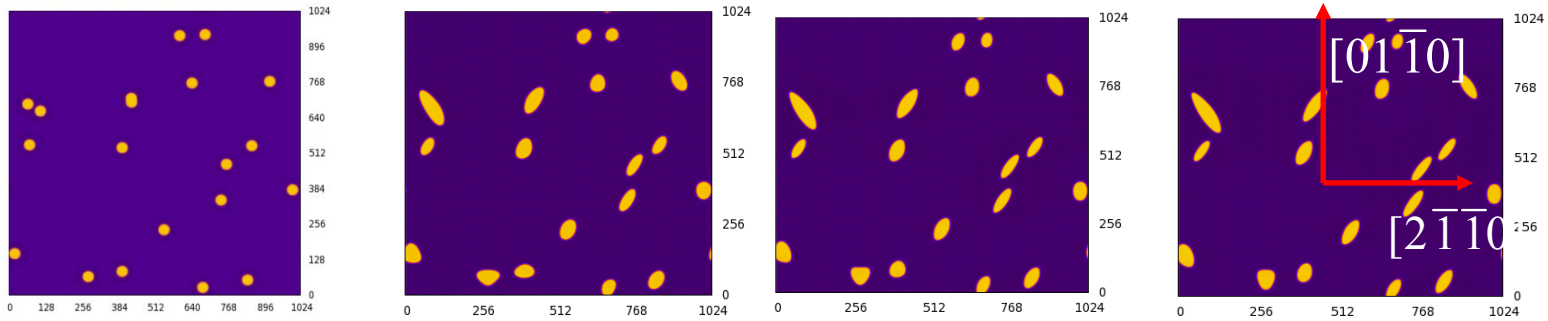

τ=1 τ=10k τ=15k τ=20k

600MPa

600MPa

Applied Stress

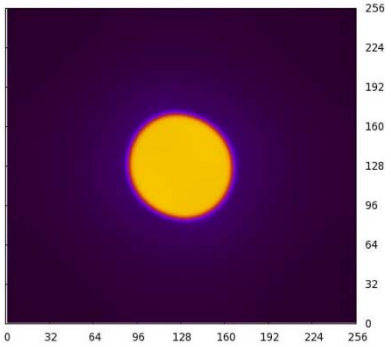

τ=1000

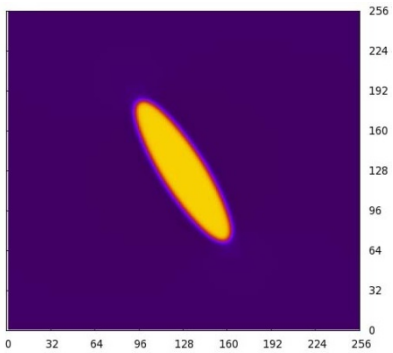

τ=20000

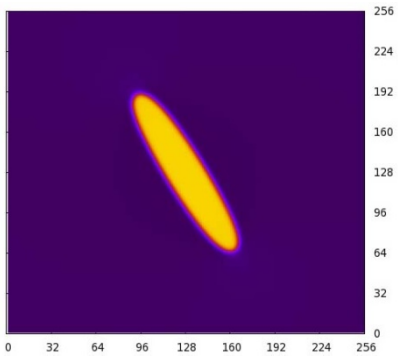

τ=100k

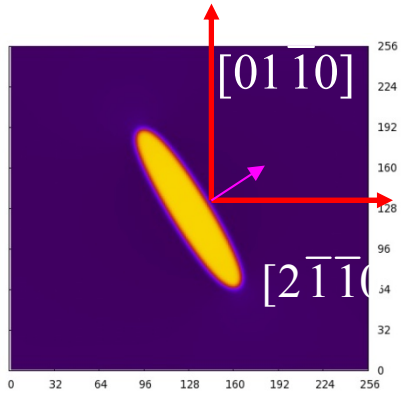

τ=200k

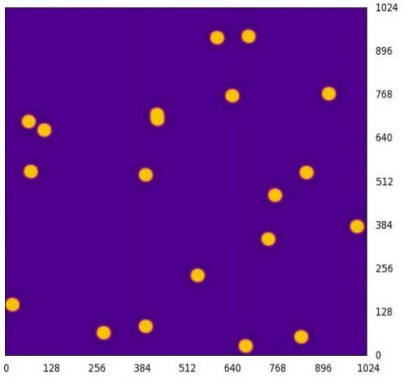

τ=100

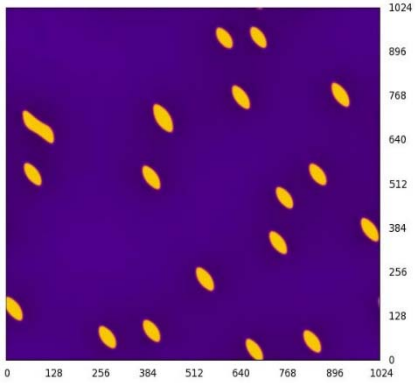

τ=5000

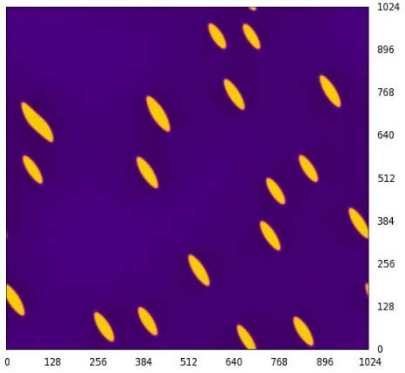

τ=10000

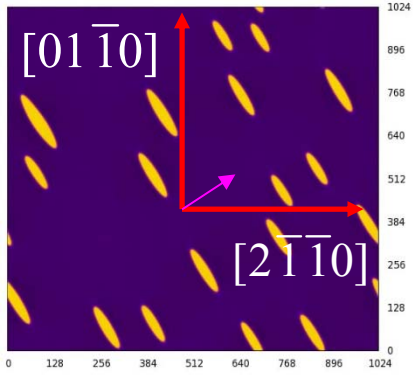

τ=25000

80MPa

Applied Stress

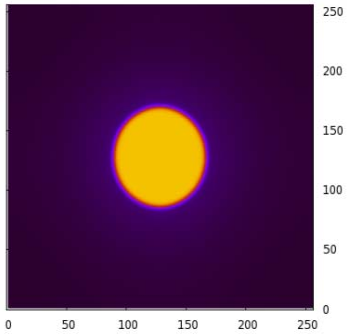

τ=1000

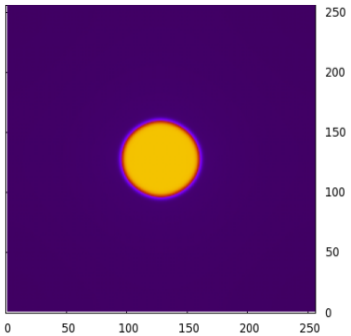

τ=10000

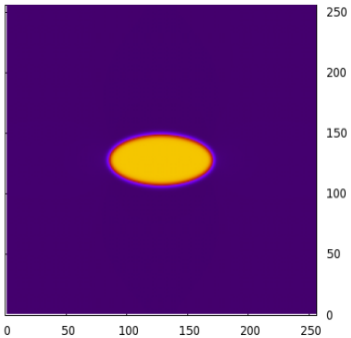

τ=60000

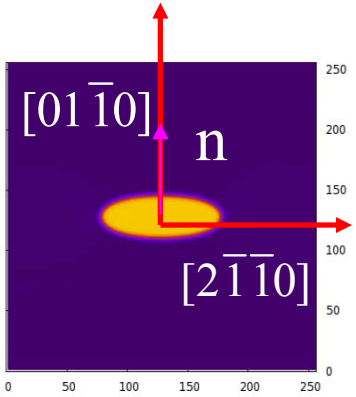

τ=135000

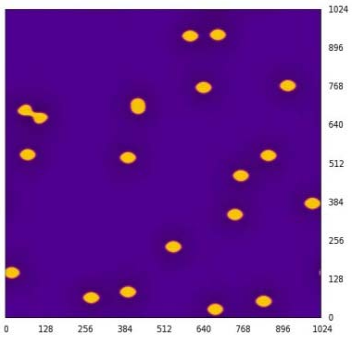

τ=1000

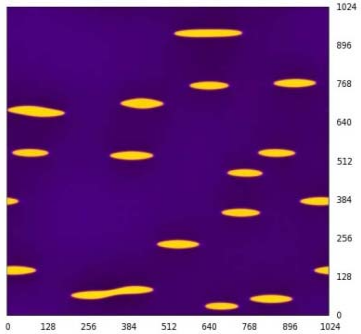

τ=1000

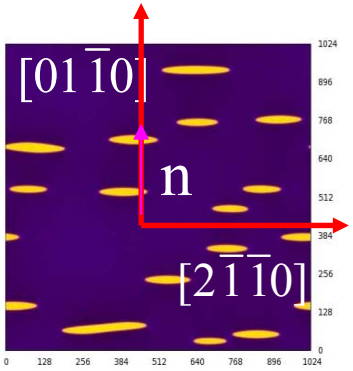

τ=15000

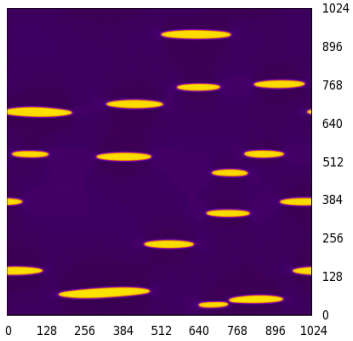

τ=25000

In summary:

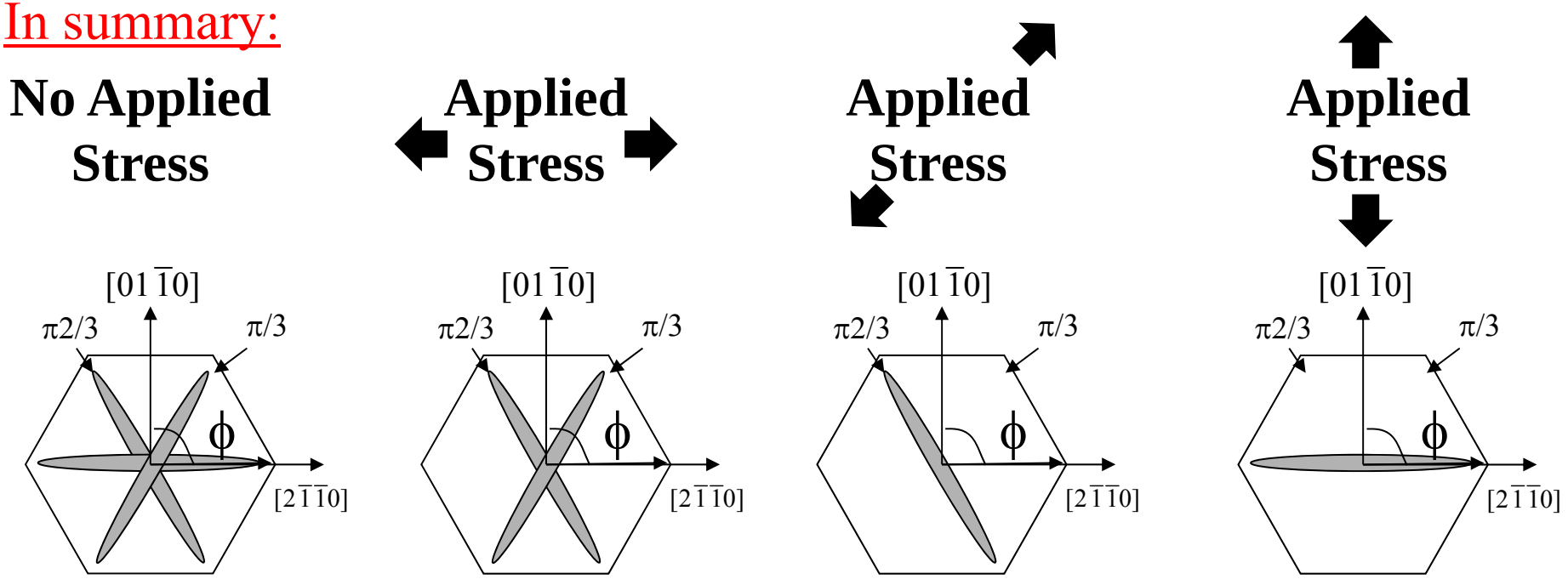

✓The level of the critical stress to apply to trigger reorientation depends on:

- The volume fraction of precipitates
- The interfacial energy of precipitates
- The orientation of the applied load

(Thuinet et al, JNM 2013)

Application 2:

Calculation of sink strengths

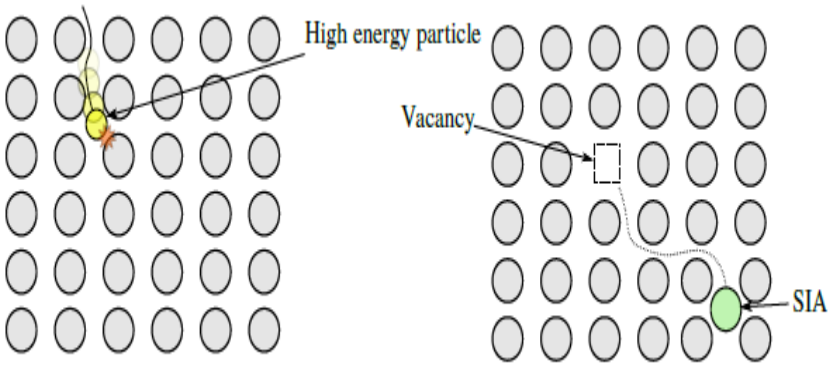

Frenkel pair formation

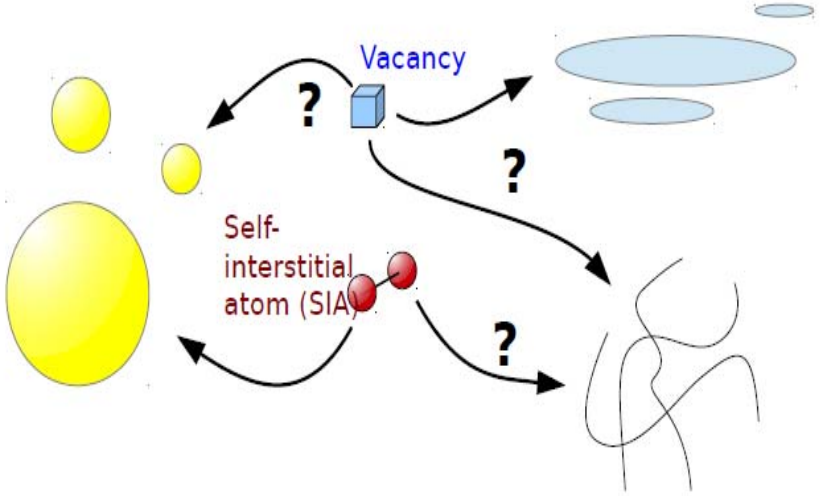

Multi-sink interactions

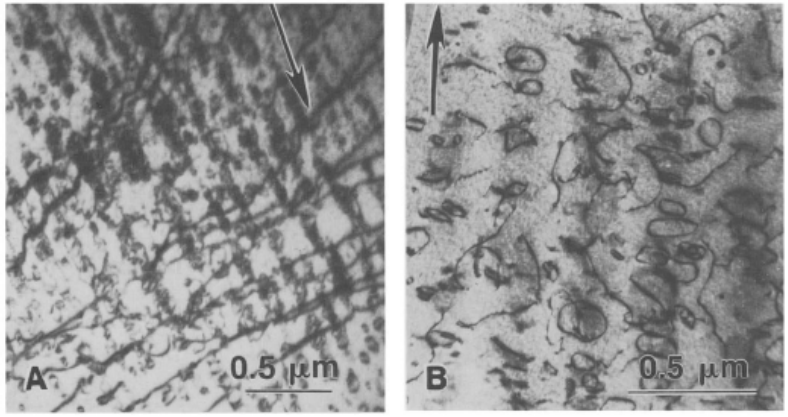

<a> loops in Zr

Methodology

$$\frac{\partial X}{\partial t}(\boldsymbol{r},t) = D\nabla^2 X + \frac{D}{k_B T}\nabla\left[X\nabla\mu_{el}\right] + K_0 - J^{sink}$$

"Fick-type" term

Elastic interaction

Irradiation PD generation rate

PD absorption by sinks

μ_{el} is computed with the **microelasticity theory** developed by Khachaturyan, it depends on:

- **Microstructure** defined by order parameters
- **Elastic constants** of the system
- **Stress free strain** ε_{ij}^{η} associated with the **dislocation**
- **Vegard's coefficients** ε_{ij}^{SIA} , ε_{ij}^{V} associated with **PD formation**

(H. Rouchette et al Computational Materials Science 88 pp. 50-60 (2014))

$$\frac{\partial X}{\partial t}(\boldsymbol{r},t) = D\nabla^2 X + \frac{D}{k_B T}\nabla\left[X\nabla\mu_{el}\right] + K_0 - J^{sink}$$

PD absorption by sinks

"Fick-type" term

Elastic interaction

Irradiation PD generation rate

Compute dislocation loop stress field

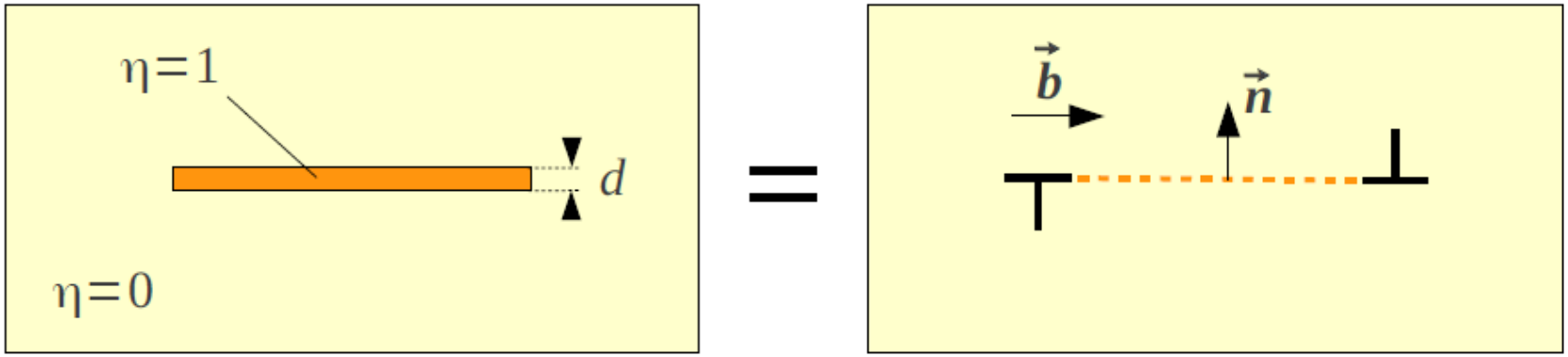

Platelet stress-free strain

$$\varepsilon_{ij}^{\eta} = \frac{1}{2d}\left(b_i n_j + b_j n_i\right)$$

Burgers vector

Normal to habit plane

F. Nabarro, *Theory of Crystal Dislocations*, Clarendon Press, Oxford, England, 1967.

Y. Wang, Y. Jin, A. Cuitino A. Khachaturyan, Acta Mater. 49 (2001) 1847–1857.

$$\frac{\partial X}{\partial t}(\boldsymbol{r},t) = \boxed{D\nabla^2 X} + \boxed{\frac{D}{k_B T}\nabla\left[X\nabla\mu_{el}\right]} + \boxed{K_0 - J^{sink}}$$

PD absorption by sinks

"Fick-type" term

Elastic interaction

Irradiation PD generation rate

Uniform irradiation + local absorption

$$J^{sink} = \lambda_{eff}\lambda(\boldsymbol{r}).(X(\boldsymbol{r}) - X_{eq})$$

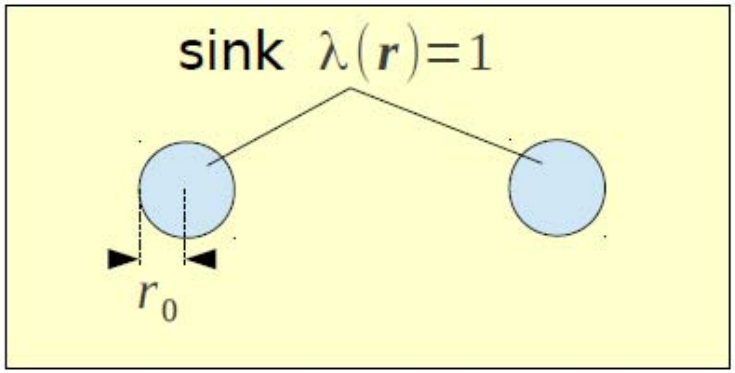

Straight dislocation case

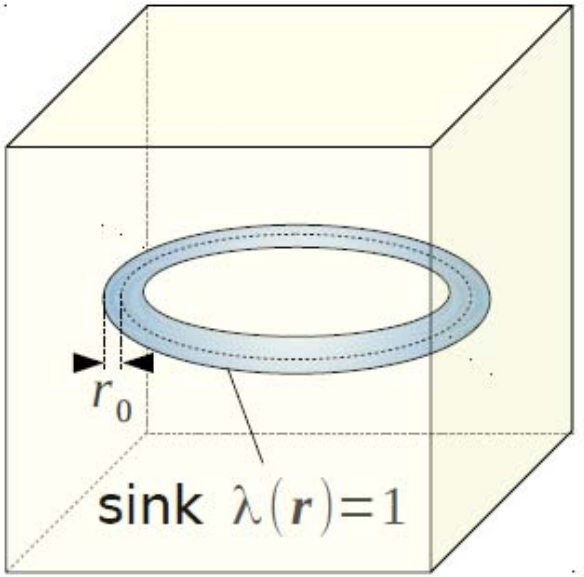

Dislocation loop case

Sink efficiency calculation method

→ Until steady state

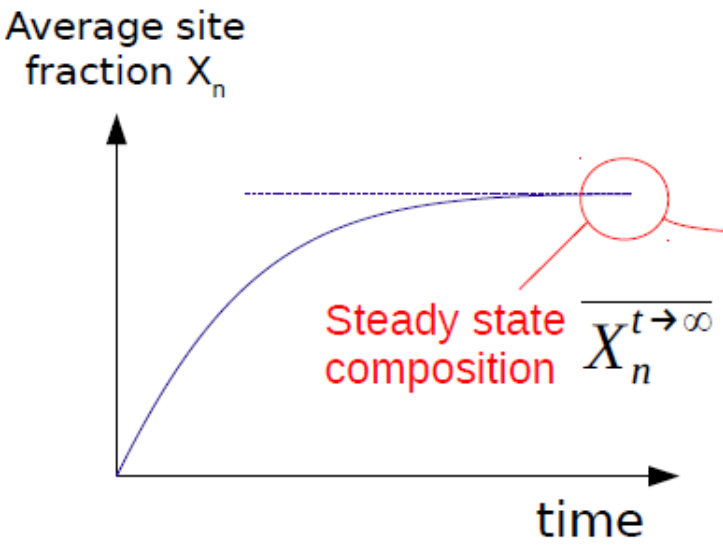

→ Deduce **sink efficiency Z:**

$$Z_s^n = \frac{J_s^n}{\rho_s . D_n . \overline{X_n^{t\to\infty}}}$$

Input variable

Computed by PF model

Absorption bias:

$$B_s = \frac{Z_s^i - Z_s^v}{Z_s^i}$$

If $B_1 > B_2$: $J_1^{SIA} > J_1^{vac}$; $J_2^{SIA} < J_2^{vac}$

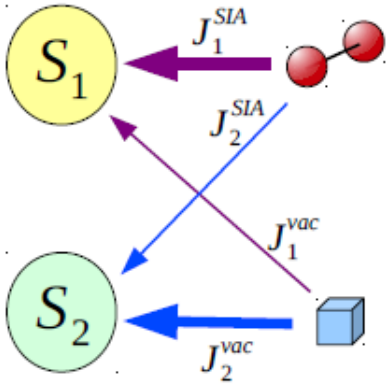

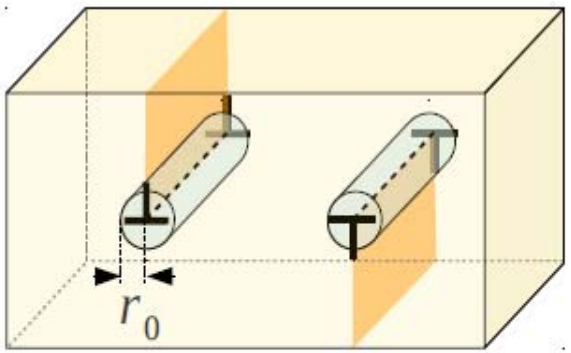

Zirconium properties

$T = 600\,K$
$r_0 = 1.13\,nm$
$a_0 = 0.323\,nm$

$C_{11} = 155\,GPa$
$C_{12} = 67\,GPa$
$C_{13} = 65\,GPa$
$C_{33} = 173\,GPa$
$C_{44} = 36\,GPa$

$\varepsilon_{aa}^{SIA} = +0.55$
$\varepsilon_{cc}^{SIA} = +0.05$
$\varepsilon_{aa}^{V} = -0.13$
$\varepsilon_{cc}^{V} = -0.18$

Obtained *Ab initio*

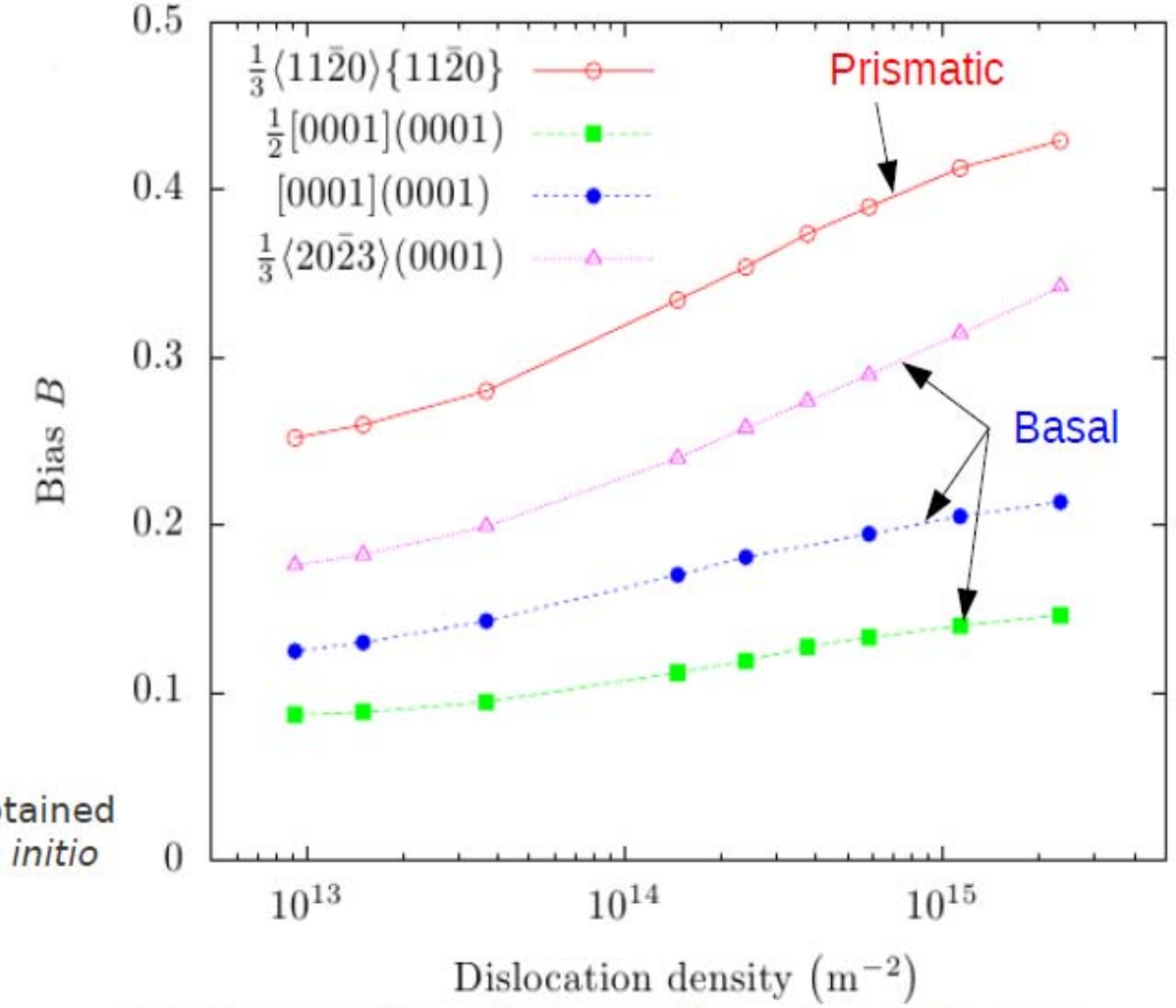

Prismatic dislocation lines have **higher bias than basal** dislocations

→ due to **SIA anisotropy**

G. Vérité et al., Phys. Rev. B **87**, 134108 (2013)

(Rouchette et al, PRB 90, 014104 (2014))

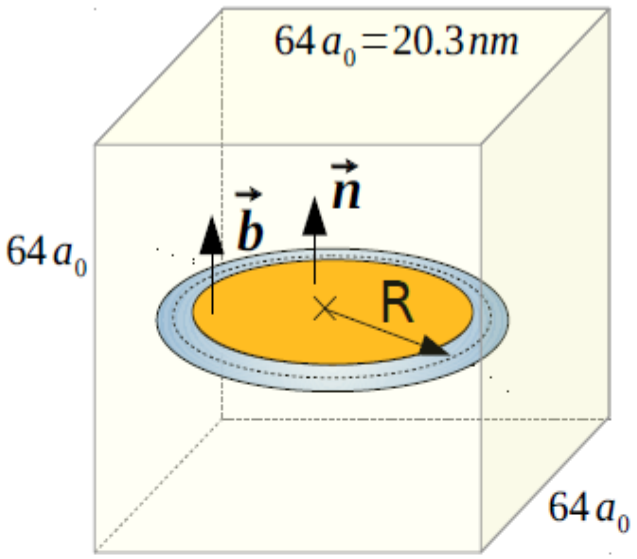

$V_{at} = 2.3 \times 10^{-29}\,m^3$

$\varepsilon_{ij}^{SIA} = +0.15\,\delta_{ij}$

$\mu = 33\,GPa$

$\nu = 0.33$

} Isotropic properties

$T = 600\,K$

$r_0 = 1.04\,nm$

$N_L = 1.13 \times 10^{23}\,m^{-3}$

$b = 0.323\,nm$

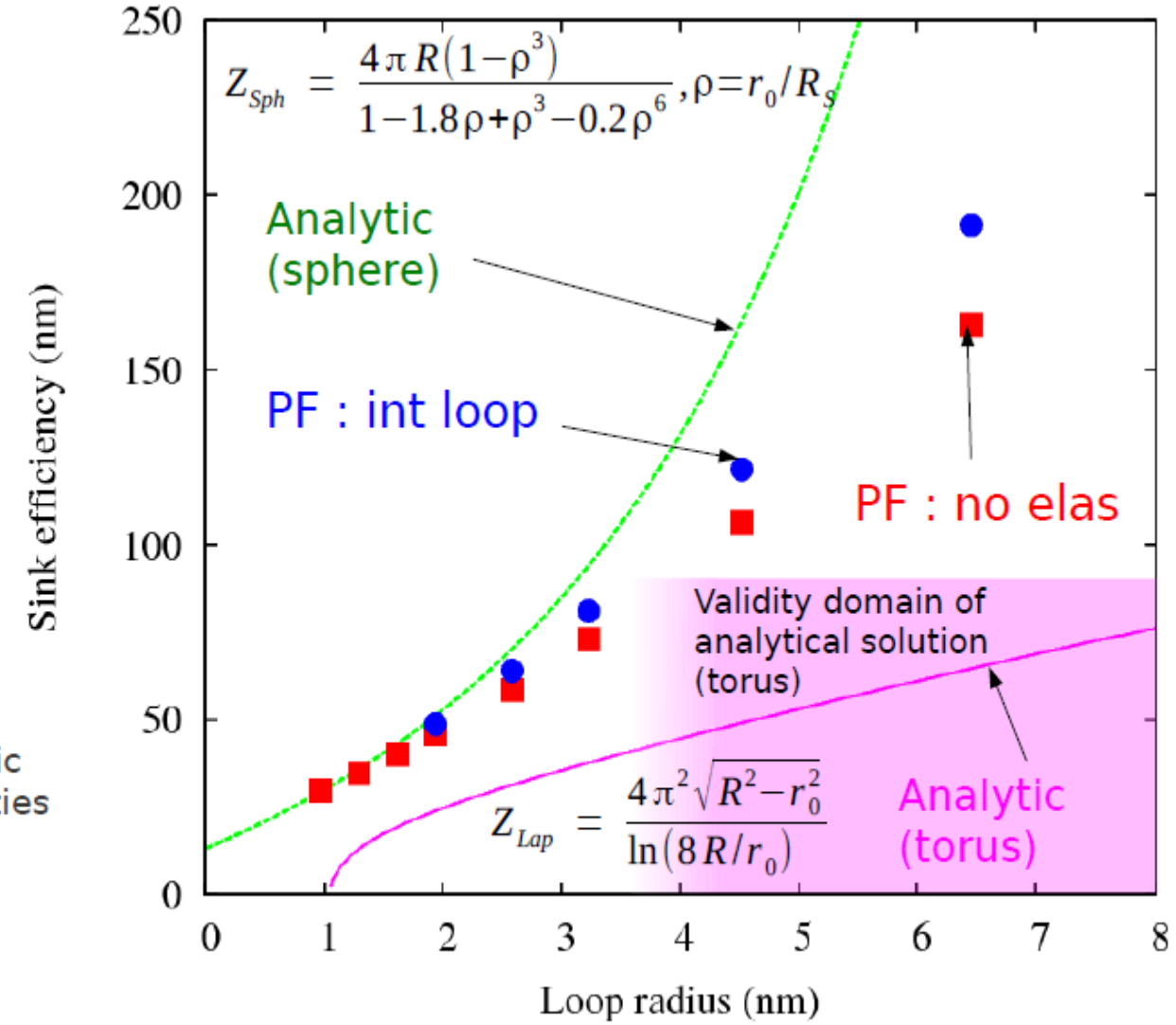

(H. Rouchette et al, Nucl. Inst. and Meth. in Physics Res. Sec.B (2015))

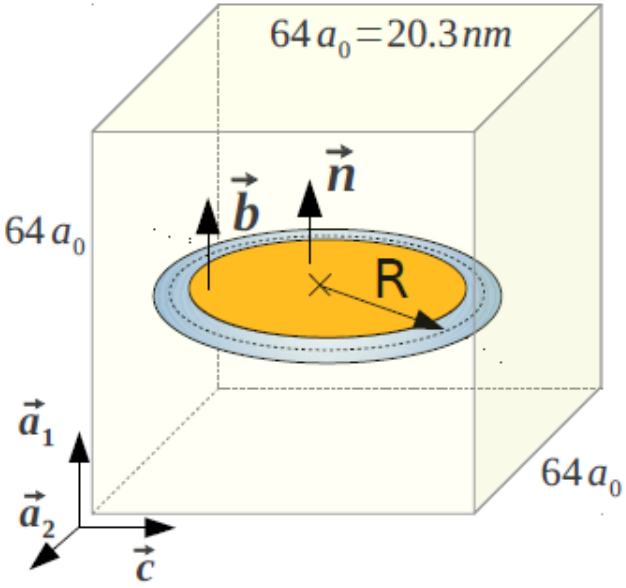

$$B = \frac{Z^i - Z^v}{Z^i}$$

Absorption bias B

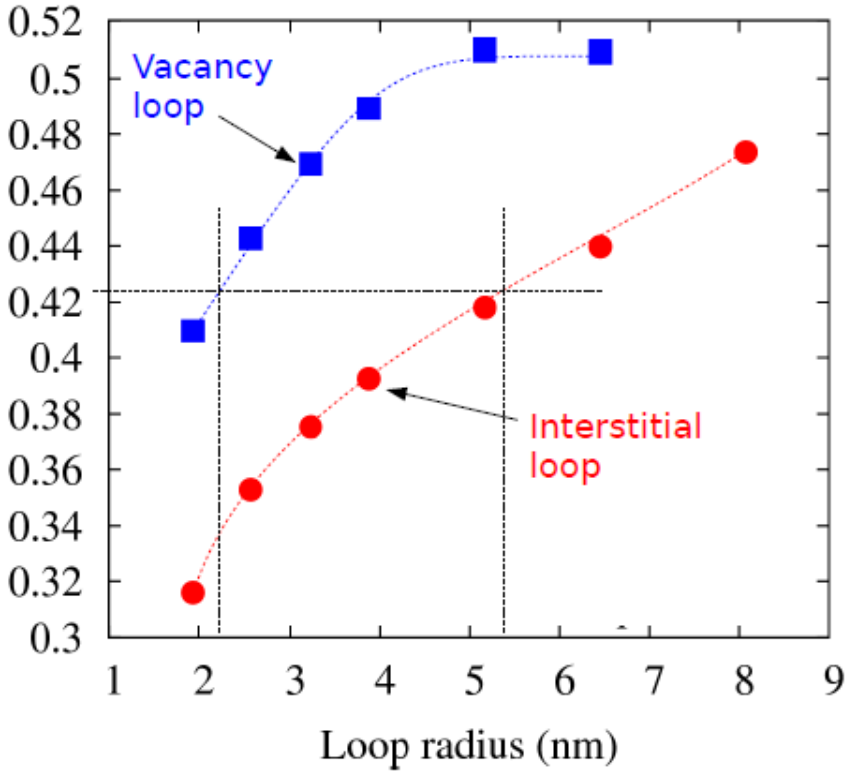

Zirconium properties

$N_L = 1.13 \times 10^{23} m^{-3}$
$T = 600\,K$
$r_0 = 1.13\,nm$
$b = 0.323\,nm$
$a_0 = b$

$C_{11} = 155\,GPa$
$C_{12} = 67\,GPa$
$C_{13} = 65\,GPa$
$C_{33} = 173\,GPa$
$C_{44} = 36\,GPa$

$\varepsilon_{aa}^{SIA} = +0.55$
$\varepsilon_{cc}^{SIA} = +0.05$
$\varepsilon_{aa}^{V} = -0.13$
$\varepsilon_{cc}^{V} = -0.18$

$Zr, 10^{23} n.m^{-2}, T = 573\mathrm{K}:$
$N_L \approx 10^{22} m^{-3}, 1 < R < 10\mathrm{nm}$

A. Jostsons et al., Jour. Nucl. Mater **66** (1977) 236-256

Loop nature has a strong influence on bias

According to these results, **cohabitation is only possible if interstitial loops** are **much larger than vacancy loops**

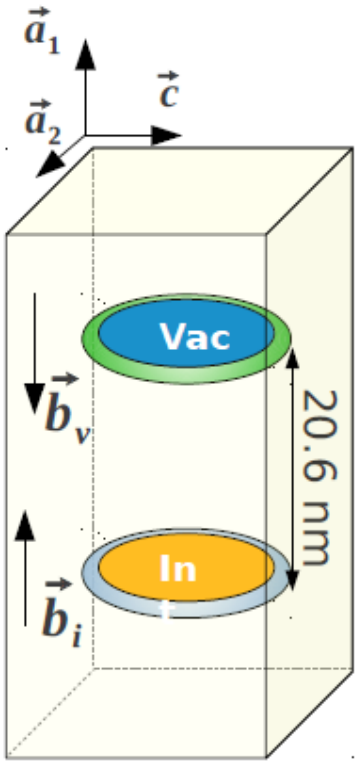

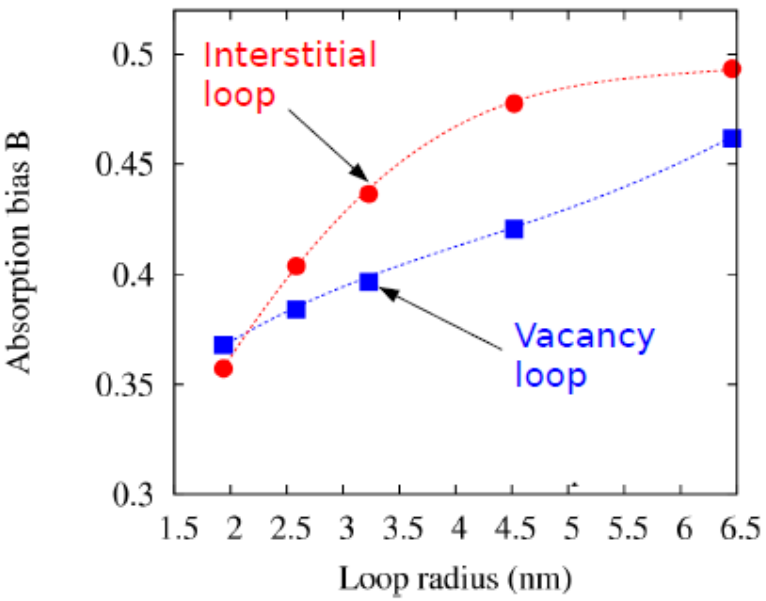

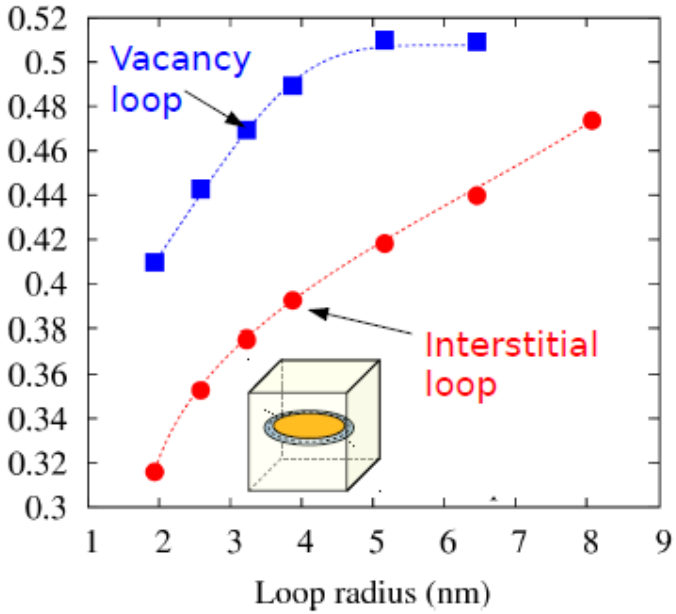

$N_L = 1.13 \times 10^{23}\, m^{-3}$

Zirconium properties as input

Elastic interaction between interstitial and vacancy loops:

➔ **Higher bias** for **interstitial loops**

➔ **Lower bias** for **vacancy loops**

➔ **Promotes growth of both vacancy and interstitial loops** in comparison with previous computation

Application 3:

Radiation Induced Segregation

Formalism

Fe-9Cr irradiated at 3 dpa, 1E-7 dpa.s^{-1}, 500°C

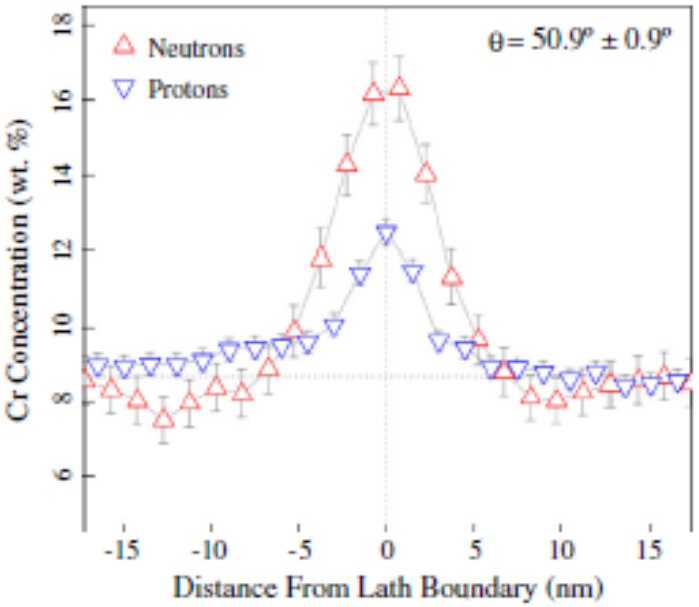

K. G. Field, Journal of Nuclear Materials 445 (2014) 143–148

Vacancies	$\frac{\partial X_V}{\partial t}(r,t) = -\nabla \cdot J_V + K_0 - K_V^{abs}(r,t) - K_R$
Interstitials	$\frac{\partial X_I}{\partial t}(r,t) = -\nabla \cdot J_I + K_0 - K_I^{abs}(r,t) - K_R$
Atoms: Fe/Cr	$\frac{\partial X_\alpha}{\partial t}(r,t) = -\nabla \cdot J_\alpha$

Diffusion

- $J_\alpha = J_\alpha^V + J_\alpha^I$
- $J_V = -J_\alpha^V - J_\beta^V$
- $J_I = J_\alpha^I + J_\beta^I$
- $J_\alpha^V = -L_{\alpha\alpha}^V(\nabla\mu_\alpha - \nabla\mu_V) - L_{\alpha\beta}^V(\nabla\mu_\beta - \nabla\mu_V)$
- $J_\alpha^I = -L_{\alpha\alpha}^I(\nabla\mu_\alpha + \nabla\mu_I) - L_{\alpha\beta}^I(\nabla\mu_\beta + \nabla\mu_I)$

Creation

- $K_0 = 1E-5\ dpa \cdot s^{-1}$

Recombination

- $K_R = RX_VX_I$

Absorption

- $K_d^{abs} = \lambda(r)\lambda_{eff}(X_d(r,t) - X_d^S)$

Coupling between atomic and mesoscale

property	coefficient	calculation
Onsager coefficients	$\begin{pmatrix} L^V_{FeFe} & L^V_{FeCr} \\ L^V_{FeCr} & L^V_{CrCr} \end{pmatrix}$ and $\begin{pmatrix} L^I_{FeFe} & L^I_{FeCr} \\ L^I_{FeCr} & L^I_{CrCr} \end{pmatrix}$	Kinetic MC ➢ Einstein equation
Thermal fraction of point defects	X_V^{eq} and X_I^{eq}	Kinetic MC
Thermodynamic factor	Φ	Metropolis MC ➢ Widom-type substitution technique
Stiffness parameter	κ	Mean field theory ➢ Mixing energy computed with MC potential

- Irradiation rate: $1E-5$ dpa $\cdot s^{-1}$
- Sink density: 1E9 m^{-1}
- Point defect fractions at grain boundary (GB): 0

Cr Depletion:
Fe-0.15Cr at 800 K

Cr Enrichment:
Fe-0.1Cr at 700 K

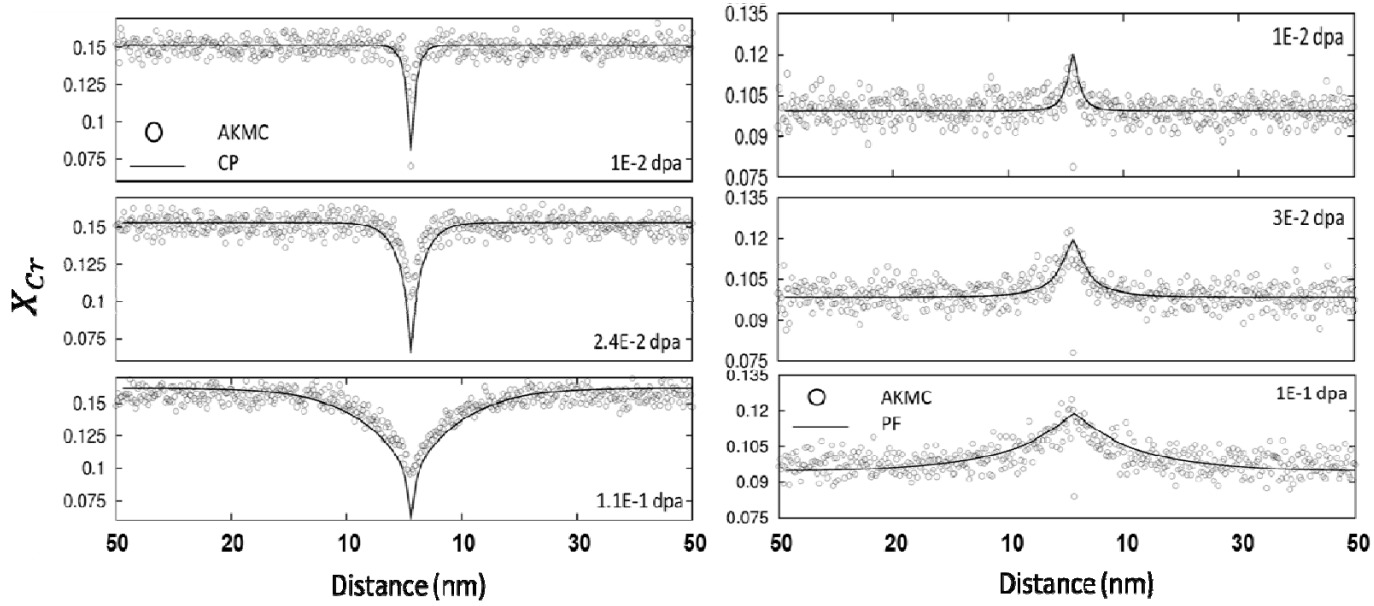

Piochaud et al, MRS 2015

Validation… and beyond

- Irradiation rate: $1E-5\ \mathrm{dpa}\cdot s^{-1}$
- Sink density: $1E7\ m^{-1}$
- Point defect fractions at GB: 0

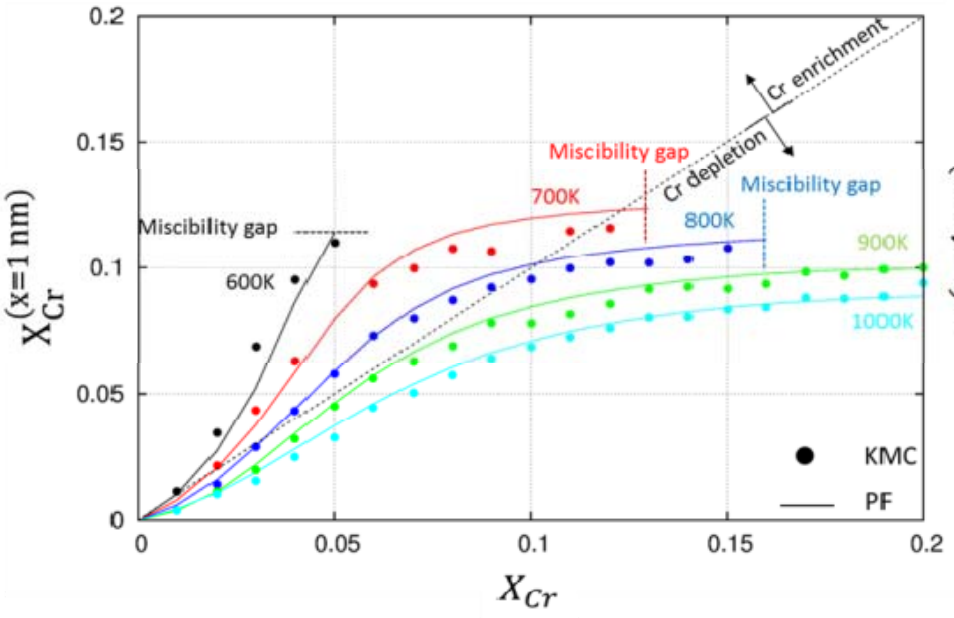

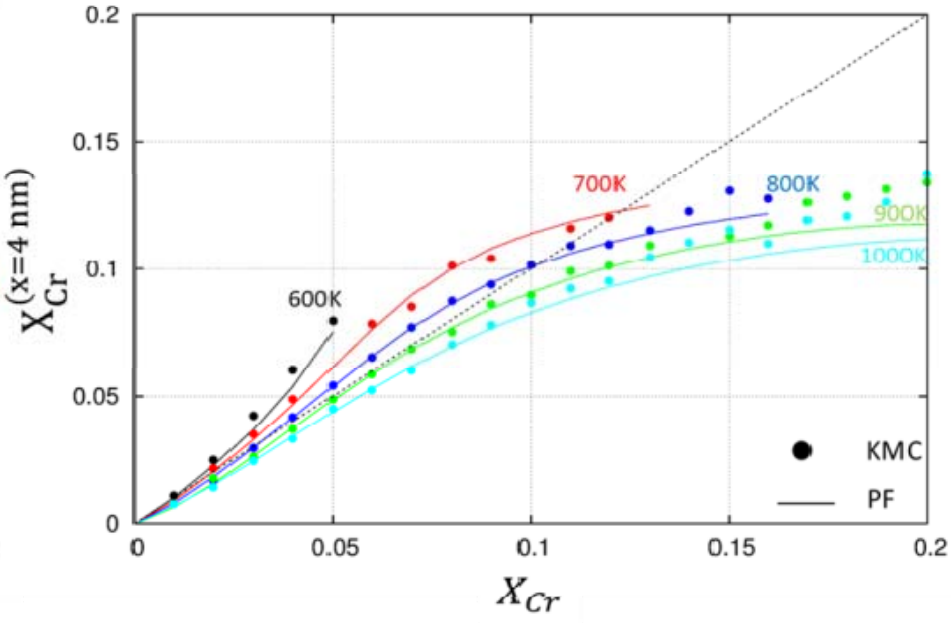

✓Virtual numerical experiences: thermodynamics is changed but not kinetics

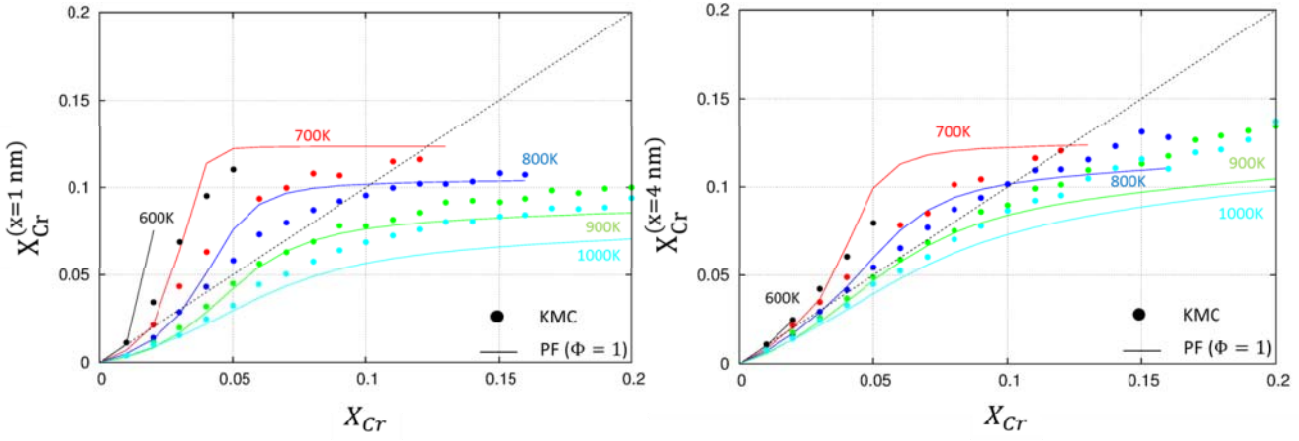

✓Influence of the composition at the grain boundary

- Sink density: 1E7 m^{-1}
- Thermal fractions of point defects at GB

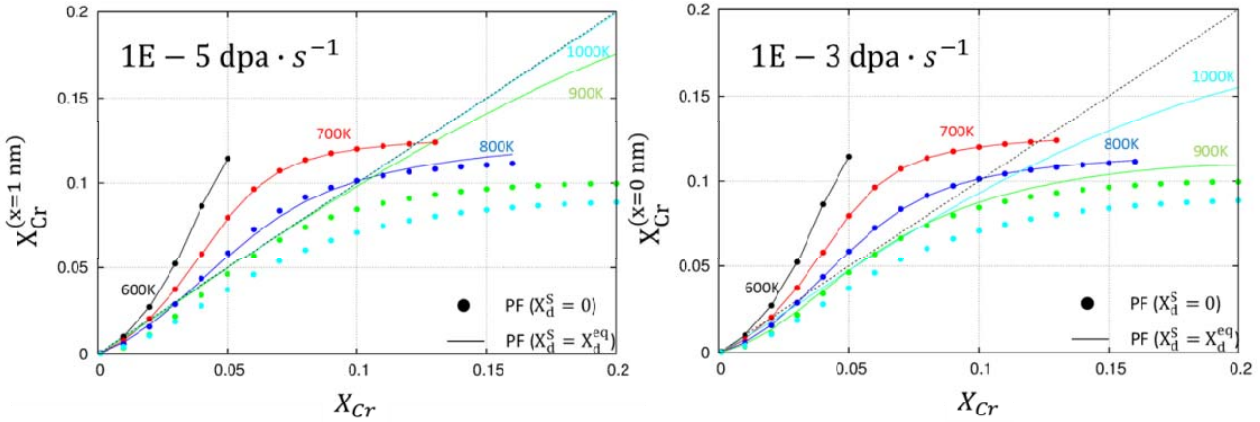

What have we learnt?

✓Phase-field models are built following 3 main steps:
1/ Definition of the order parameters
2/ Definition of the energy functional
3/ Definition of the kinetic equations

✓Phase-field models can deal with the evolution of arbitrary morphologies and complex microstructures without explicitly tracking the positions of interfaces.

✓Microelasticity theory can be easily incorporated in the phase-field formalism. Then, long-range elastic interactions between phases, dislocations, diffusing species can be taken into account.

✓Phase-field models have been successfully applied to various materials processes including solidification, solid-state phase transformations, coarsening, and growth. Significant additional efforts are still required to couple these approaches with macroscopic models.